

# Study of $B_s \rightarrow \phi \ell^+ \ell^-$ decays in the PQCD factorization approach with lattice QCD input

Su-Ping Jin<sup>1\*</sup> and Zhen-Jun Xiao<sup>1,2†</sup>

1. *Department of Physics and Institute of Theoretical Physics, Nanjing Normal University, Nanjing, Jiangsu 210023, People's Republic of China, and*

2. *Jiangsu Key Laboratory for Numerical Simulation of Large Scale Complex Systems, Nanjing Normal University, Nanjing 210023, People's Republic of China*

(Dated: February 2, 2021)

In this paper, we studied systematically the semileptonic decays  $B_s \rightarrow \phi \ell^+ \ell^-$  with  $\ell^- = (e^-, \mu^-, \tau^-)$  by using the perturbative QCD (PQCD) and the “PQCD+Lattice” factorization approach, respectively. We first evaluated all relevant form factors  $F_i(q^2)$  in the low  $q^2$  region using the PQCD approach, and we also took the available lattice QCD results at the high- $q^2$  region as additional input to improve the extrapolation of  $F_i(q^2)$  from the low- $q^2$  region to the endpoint  $q_{max}^2$ . We then calculated the branching ratios and many other physical observables:  $A_{FB}(\ell)$ ,  $F_L^\phi$ ,  $S_{3,4,7}$ ,  $A_{5,6,8,9}$  and the clean angular observables  $P_{1,2,3}$  and  $P'_{4,5,6,8}$ . From our studies, we find the following points: (a) the PQCD and “PQCD+Lattice” predictions of  $\mathcal{B}(B_s \rightarrow \phi \mu^+ \mu^-)$  are about  $7 \times 10^{-7}$ , which agree well with the LHCb measured value and the QCD sum rule prediction within one standard deviation; (b) we defined and calculated the ratios of the branching ratios  $R_\phi^{e\mu}$  and  $R_\phi^{\mu\tau}$ ; (c) the PQCD and “PQCD+Lattice” predictions of the longitudinal polarization  $F_L$ , the CP averaged angular coefficients  $S_{3,4,7}$  and the CP asymmetry angular coefficients  $A_{5,6,8,9}$ , agree with the LHCb measurements in all considered bins within the still large experimental errors; and (d) for those currently still unknown observables  $R_\phi^{e\mu}$ ,  $R_\phi^{\mu\tau}$ ,  $A_{FB}^\ell$ ,  $P_{1,2,3}$  and  $P'_{4,5,6,8}$ , we suggest LHCb and Belle-II Collaboration to measure them in their experiments.

PACS numbers: 13.20.He, 12.38.Bx, 14.40.Nd

## I. INTRODUCTION

In the Standard Model (SM) of particle physics, one treats these three generations of the charged leptons  $\ell^- = (e^-, \mu^-, \tau^-)$  as exact copies of each other. These charged leptons behave in the same way but differ only in the masses determined by their Yukawa coupling to the Higgs boson. The lepton flavor universality (LFU), i.e. the equality of the coupling to the all electroweak gauge bosons among three families of leptons, has been regarded as an exact symmetry for quite a long time[1]. In recent years, however, some physics observables associated with the flavor-changing neutral current (FCNC) transitions  $b \rightarrow s \ell \ell$  have exhib-

\*Electronic address: [2223919088@qq.com](mailto:2223919088@qq.com)

†Electronic address: [xiaozhenjun@njnu.edu.cn](mailto:xiaozhenjun@njnu.edu.cn); Corresponding author

ited deviations from the SM expectations. These include the LFU-violating(LFUV) ratios  $R_K$  and  $R_{K^*}$  [2, 3], whose measurements deviates from  $\mu - e$  universality [4–6] by around  $2.5\sigma$ . More notably, the measurements of the angular observable  $P'_5$  of  $B \rightarrow K^* \mu^+ \mu^-$  decay in the large recoil region [7–11] as reported by the LHCb [12, 13] and Belle Collaboration [14] point to a deviation of about  $3\sigma$  with respect to the SM prediction [15].

As is well known, the FCNC  $b \rightarrow s$  transition is forbidden at tree-level, but proceeds by way of loop diagrams with a very low rate. Due to the strong suppression within SM, such kinds of FCNC decays may be sensitive to the possible new physics (NP) effects. Therefore, the semileptonic  $b \rightarrow s \ell \ell$  decay has received striking attentions by means of measurements of the inclusive  $B \rightarrow X_s \ell^+ \ell^-$  and/or the exclusive  $B \rightarrow K^{(*)} \ell^+ \ell^-$  decays and their comparison with the SM predictions. Besides the decay rates, many angular observables of the semileptonic  $B \rightarrow K^* \mu^+ \mu^-$  decays have also been measured previously [12–14]. The precision of the experimental measurements will also be expected to upgrade remarkably in the forthcoming year.

The semileptonic decay  $B_s \rightarrow \phi \mu^+ \mu^-$ , which is closely relevant to the decay  $B \rightarrow K^* \mu^+ \mu^-$ , offers an alternative scene to check out the same fundamental quark process, in a different hadronic background. On the theoretical side, various studies on the quark level  $b \rightarrow s$  transition and the exclusive  $B_{(s)} \rightarrow V \ell^+ \ell^-$  decays by using rather different theories or models have been performed within the SM, such as the constituent quark model or covariant quark model [16, 17], the light front quark model [18], the QCD factorization (QCDF) [19] and the light-cone sum rule (LCSR) [20–25], and beyond the SM, such as the universal extra dimension [26, 27] and the supersymmetric theory [28]. On the experimental side, the  $B_s \rightarrow \phi \mu^+ \mu^-$  decay mode was first observed and studied by the CDF collaboration [29] and subsequently by the LHCb collaboration [30, 31]. Beyond the measurement of the branching ratio, a rich phenomenology of various kinematical distributions can be presented. While the angular distributions was found to be consistent with the SM expectations obtained in Refs. [22, 23], however, LHCb also observed a deficit with respect to the SM prediction for the branching ratio  $B_s^0 \rightarrow \phi \mu^+ \mu^-$  in the low- $q^2$  region: the tension between the theory and experiment is about  $3\sigma$  in the region  $1.0 \leq q^2 \leq 6.0 \text{ GeV}^2$ , where the form factors are evaluated by using the combined fit of lattice and the LCSR results [22, 23].

In a previous paper [32], the semileptonic  $B_s \rightarrow K^{(*)} \ell^+ \ell^-$  decays have been studied by us using the perturbative QCD (PQCD) factorization approach [33–45]. In this paper, we will make systematic studies for the semileptonic  $B_s \rightarrow \phi \ell^+ \ell^-$  and present the theoretical predictions for many physical observables:

- (1) For  $B_s \rightarrow \phi \ell^+ \ell^-$  decays, we treat them as a four body decay  $B_s \rightarrow \phi(\rightarrow K^- K^+) \ell^+ \ell^-$  described by four kinematic variables: the lepton invariant mass squared  $q^2$  and three angles  $(\theta_K, \theta_\ell, \Phi)$ . We defined and calculated the full angular decay distribution, the transverse amplitudes, the partially integrated decay amplitudes over the angles  $(\theta_K, \theta_\ell, \Phi)$ , the CP averaged differential branching, the ratios  $R^{e\mu}(\phi)$  and  $R^{\mu\tau}(\phi)$  of the branching ratios, the forward-backward asymmetry  $A_{FB}(q^2)$ , the  $\phi$  polarization fraction  $F_L(q^2)$ , the CP averaged (asymmetry) angular coefficients  $S_i$  ( $A_i$ ) and the optimized observables  $P_i$  and  $P'_i$ . Here, when considering the branching fractions we take the S-wave correction as an additional uncertainty, the size of which is set to 5% conservatively.
- (2) We used both the PQCD factorization approach and the “PQCD+Lattice” approach to determine the values and their  $q^2$ -dependence of the  $B_s \rightarrow \phi$  transition form fac-

tors. We used the  $z$ -series parametrization to make the extrapolation for all form factors from the low  $q^2$  region to the endpoint  $q_{max}^2$ . We will calculate the branching ratios and all other physical observables by using the PQCD approach itself and the “PQCD+Lattice” approach respectively, and compare their predictions with those currently available experimental measurements.

The paper is organized as follows: In Sec. II, we give a short review for the kinematics of the  $B_s \rightarrow \phi \ell^+ \ell^-$  decays including distribution amplitudes of  $B_s$  and  $\phi$  mesons, and the effective Hamiltonian for the quark level  $b \rightarrow s \ell^+ \ell^-$ . In Sec. III, we define explicitly all physical observables for  $B_s \rightarrow \phi \ell^+ \ell^-$  decays. In Sec. IV we present our theoretical predictions of all relevant physical observables of the considered decay modes, compare these predictions with those currently available experimental measurements and make some phenomenological analysis. A short summary is given in the last section.

## II. KINEMATICS AND THEORETICAL FRAMEWORK

### A. Kinematics and wave functions

We treat the  $B_s$  meson at rest as a heavy-light system. The kinematics of the semileptonic  $B_s \rightarrow \phi \ell^+ \ell^-$  decays in the large-recoil (low  $q^2$ ) region will be discussed below, where the PQCD factorization approach is applicable to the considered decays. In the rest frame of  $\bar{B}_s^0$  meson, we define the  $\bar{B}_s^0$  meson momentum  $p_1$ , the  $\phi$  momentum  $p_2$  in the light-cone coordinates as Ref. [38]. We also use  $x_i$  to denote the momentum fraction of light anti-quark in each meson and set the momentum  $p_i$  and  $k_i$  ( the momenta carried by the spectator quark in  $B_s$  and  $\phi$  meson ) in the following forms:

$$\begin{aligned} p_1 &= \frac{m_{B_s}}{\sqrt{2}}(1, 1, 0_\perp), \quad p_2 = \frac{r m_{B_s}}{\sqrt{2}}(\eta^+, \eta^-, 0_\perp), \\ k_1 &= (0, x_1 \frac{m_{B_s}}{\sqrt{2}}, k_{1\perp}), \quad k_2 = \frac{m_{B_s}}{\sqrt{2}}(x_2 r \eta^+, x_2 r \eta^-, k_{2\perp}). \end{aligned} \quad (1)$$

where the mass ratio  $r = m_\phi/m_{B_s}$ , and the factor  $\eta^\pm$  is defined in the following form:

$$\eta^\pm = \eta \pm \sqrt{\eta^2 - 1}, \quad \text{with} \quad \eta = \frac{1}{2r} \left[ 1 + r^2 - \frac{q^2}{m_{B_s}^2} \right], \quad (2)$$

where  $q = p_1 - p_2$  is the lepton-pair four-momentum. For the final state  $\phi$  meson, its longitudinal and transverse polarization vector  $\epsilon_{L,T}$  can be written in the form of  $\epsilon_L = (\eta^+, -\eta^-, 0_\perp)/\sqrt{2}$  and  $\epsilon_T = (0, 0, 1)$ .

For the  $B_s$  meson wave function, we use the same kind of parameterizations as in Refs. [39, 40]

$$\Phi_{B_s} = \frac{i}{\sqrt{2N_c}} (\not{p}_{B_s} + m_{B_s}) \gamma_5 \phi_{B_s}(k_1). \quad (3)$$

Here only the contribution of the Lorentz structure  $\phi_{B_s}(k_1)$  is taken into account, since the contribution of the second Lorentz structure  $\bar{\phi}_{B_s}$  is numerically small and has been

neglected. We adopted the distribution amplitude of the  $B_s$  meson in the similar form as that of  $B$ -meson in the  $SU(3)_f$  limit being widely used in the PQCD approach

$$\phi_{B_s}(x, b) = N_{B_s} x^2 (1-x)^2 \exp \left[ -\frac{m_{B_s}^2 x^2}{2\omega_{B_s}^2} - \frac{1}{2}(\omega_{B_s} b)^2 \right]. \quad (4)$$

In order to estimate the theoretical uncertainties induced by the variations of  $\phi_{B_s}(x, b)$ , one usually take  $\omega_{B_s} = 0.50 \pm 0.05$  GeV for  $B_s^0$  meson. The normalization factor  $N_{B_s}$  depends on the values of the shape parameter  $\omega_{B_s}$  and the decay constant  $f_{B_s}$  and defined through the normalization relation :  $\int_0^1 dx \phi_{B_s}(x, 0) = f_{B_s}/(2\sqrt{6})$  [40].

For the vector meson  $\phi$ , the longitudinal and transverse polarization components can both provide the contribution. Here we adopt the wave functions of the vector  $\phi$  as in Ref. [42]:

$$\Phi_\phi^\parallel(p, \epsilon_L) = \frac{i}{\sqrt{6}} [\not{\epsilon}_L m_\phi \phi_\phi(x) + \not{\epsilon}_L \not{p} \phi_\phi^t(x) + m_\phi \phi_\phi^s(x)], \quad (5)$$

$$\Phi_\phi^\perp(p, \epsilon_T) = \frac{i}{\sqrt{6}} [\not{\epsilon}_T m_\phi \phi_\phi^v(x) + \not{\epsilon}_T \not{p} \phi_\phi^T(x) + m_\phi i \epsilon_{\omega\nu\rho\sigma} \gamma_5 \gamma^\omega \epsilon_T^\nu n^\rho v^\sigma \phi_\phi^a(x)], \quad (6)$$

where  $p$  and  $m_\phi$  are the momentum and the mass of the  $\phi$  meson,  $\epsilon_L$  and  $\epsilon_T$  correspond to the longitudinal and transverse polarization vectors of the vector meson  $\phi$ , respectively. The twist-2 DAs  $\phi_\phi$  and  $\phi_\phi^T$  in Eqs. (5,6) can be reconstructed as a Gegenbauer expansion [42]:

$$\begin{aligned} \phi_\phi(x) &= \frac{3f_\phi}{\sqrt{6}} x(1-x) \left[ 1 + \sum_{n=1}^2 a_{n\phi}^\parallel C_n^{3/2}(t) \right], \\ \phi_\phi^T(x) &= \frac{3f_\phi^T}{\sqrt{6}} x(1-x) \left[ 1 + \sum_{n=1}^2 a_{n\phi}^\perp C_n^{3/2}(t) \right], \end{aligned} \quad (7)$$

where  $t = 2x - 1$ ,  $a_{1,2}^{\parallel,\perp}$  are the Gegenbauer moments, while  $C_{1,2}^{3/2}$  are the Gegenbauer polynomials as given in Ref. [42].  $f_\phi$  and  $f_\phi^T$  are the longitudinal and transverse components of the decay constants of the vector meson  $\phi$  with  $f_\phi = 0.231 \pm 0.04$  GeV and  $f_\phi^T = 0.20 \pm 0.01$  GeV as given in Ref. [42]. For the relevant Gegenbauer moments we use the same ones as those in Refs. [42–45].

$$a_1^{\parallel,\perp} = 0, \quad a_{2\phi}^\parallel = 0.18 \pm 0.08, \quad a_{2\phi}^\perp = 0.14 \pm 0.07. \quad (8)$$

The twist-3 DAs  $\phi_\phi^{s,t}$  and  $\phi_\phi^{v,a}$  in Eqs. (5,6) are the same ones as those defined in Ref. [42]:

$$\phi_\phi^t = \frac{3f_\phi^T}{2\sqrt{6}} t^2, \quad \phi_\phi^s = \frac{3f_\phi^T}{2\sqrt{6}} (-t), \quad \phi_\phi^v = \frac{3f_\phi}{8\sqrt{6}} (1+t^2), \quad \phi_\phi^a = \frac{3f_\phi}{4\sqrt{6}} (-t). \quad (9)$$

## B. Effective Hamiltonian for $b \rightarrow s\ell^+\ell^-$ decays

The semileptonic decay  $B_s \rightarrow \phi\ell^+\ell^-$  involves a  $b \rightarrow s\ell^+\ell^-$  quark-level transition. The tree-level effective Hamiltonian is not sufficient to describe the decays of interest to this thesis, as the FCNC transition only appears at loop level. This can, however, be generated

by several types of operator. The full operator set relevant to such decays is defined by the effective Hamiltonian as in Refs. [46–50]:

$$\mathcal{H}_{\text{eff}} = -\frac{4G_F}{\sqrt{2}} \left\{ V_{tb}V_{ts}^* \left[ C_1(\mu)\mathcal{O}_1^c(\mu) + C_2(\mu)\mathcal{O}_2^c(\mu) + \sum_{i=3}^{10} C_i(\mu)\mathcal{O}_i(\mu) \right] \right. \\ \left. + V_{ub}V_{us}^* \left[ C_1(\mu) [\mathcal{O}_1^c(\mu) - \mathcal{O}_1^u(\mu)] + C_2(\mu) [\mathcal{O}_2^c(\mu) - \mathcal{O}_2^u(\mu)] \right] \right\} + \text{h.c.}, \quad (10)$$

where  $G_F = 1.16638 \times 10^{-5} \text{GeV}^{-2}$  is the Fermi constant,  $V_{ij}$  are the CKM matrix elements. For the operators  $\mathcal{O}_i$  we adopt those as defined in the so-called  $\gamma_5$ -free basis [51, 52]. Following Ref. [53], the operators  $\mathcal{O}_i$  can be written in the following form:

$$\begin{aligned} \mathcal{O}_1^c &= (\bar{s}\gamma_\mu T^a P_L c)(\bar{c}\gamma_\mu T^a P_L b), & \mathcal{O}_2^c &= (\bar{s}\gamma_\mu P_L c)(\bar{c}\gamma_\mu P_L b), \\ \mathcal{O}_1^u &= (\bar{s}\gamma_\mu T^a P_L u)(\bar{u}\gamma_\mu T^a P_L b), & \mathcal{O}_2^u &= (\bar{s}\gamma_\mu P_L u)(\bar{u}\gamma_\mu P_L b), \\ \mathcal{O}_3 &= (\bar{s}\gamma_\mu P_L b)\sum_q(\bar{q}\gamma_\mu q), & \mathcal{O}_4 &= (\bar{s}\gamma_\mu T^a P_L b)\sum_q(\bar{q}\gamma_\mu T^a q), \\ \mathcal{O}_5 &= (\bar{s}\gamma_\mu\gamma_\nu\gamma_\rho P_L b)\sum_q(\bar{q}\gamma^\mu\gamma^\nu\gamma^\rho q), & \mathcal{O}_6 &= (\bar{s}\gamma_\mu\gamma_\nu\gamma_\rho T^a P_L b)\sum_q(\bar{q}\gamma^\mu\gamma^\nu\gamma^\rho T^a q), \\ \mathcal{O}_7 &= \frac{e}{g^2}m_b(\bar{s}\sigma^{\mu\nu}P_R b)F_{\mu\nu}, & \mathcal{O}_8 &= \frac{1}{g}m_b(\bar{s}\sigma^{\mu\nu}T^a P_R b)G_{\mu\nu}^a, \\ \mathcal{O}_9 &= \frac{e^2}{g^2}(\bar{s}\gamma_\mu P_L b)\sum_\ell(\bar{\ell}\gamma^\mu\ell), & \mathcal{O}_{10} &= \frac{e^2}{g^2}(\bar{s}\gamma_\mu P_L b)\sum_\ell(\bar{\ell}\gamma^\mu\gamma_5\ell). \end{aligned} \quad (11)$$

where  $\mathcal{O}_{1,2}^{c,u}$  are the current-current operators,  $\mathcal{O}_{3-6}$  are the QCD penguin operators,  $\mathcal{O}_{7,8}$  are the electromagnetic and chromomagnetic penguin operators respectively, and finally  $\mathcal{O}_{9,10}$  are the semileptonic operators. The inclusion of the factors  $4\pi/g^2 = 1/\alpha_s$  in the definition of the operators  $\mathcal{O}_{7,8,9,10}$  serves to allow a more transparent organisation of the expansion of the relevant Wilson coefficients as defined in Refs. [53, 54] up to next-to-next-to leading order (NNLO). They are then evolved from the scale  $\mu = m_W$  down to the scale  $\mu = m_b$  using the renormalization group equations.

Since the contributions from the subleading chromomagnetic penguin, quark-loop and annihilation diagrams are highly suppressed for the considered  $b \rightarrow s\ell^+\ell^-$  decays [49], we will neglect them in our calculations. Using the effective Hamiltonian in Eq. (10), the decay amplitude for  $b \rightarrow s\ell^+\ell^-$  loop transition can be decomposed as a product of a short-distance contributions through Wilson coefficients and long-distance contribution which is further expressed in terms of form factors,

$$\mathcal{A}(b \rightarrow s\ell^+\ell^-) = \frac{G_F}{\sqrt{2}} \frac{\alpha_{\text{em}}}{\pi} V_{tb}V_{ts}^* \left\{ C_9^{\text{eff}}(q^2)[\bar{s}\gamma_\mu P_L b][\bar{\ell}\gamma^\mu\ell] + C_{10}[\bar{s}\gamma_\mu P_L b][\bar{\ell}\gamma^\mu\gamma_5\ell] \right. \\ \left. - 2m_b C_7^{\text{eff}}[\bar{s}i\sigma_{\mu\nu}\frac{q^\nu}{q^2}P_R b][\bar{\ell}\gamma^\mu\ell] \right\}, \quad (12)$$

where  $C_7^{\text{eff}}(\mu)$  and  $C_9^{\text{eff}}(\mu)$  are the effective Wilson coefficients, defined as in Refs. [40, 55]

$$C_7^{\text{eff}}(\mu) = C_7(\mu) + C'_{b \rightarrow s\gamma}(\mu), \quad (13)$$

$$C_9^{\text{eff}}(\mu, q^2) = C_9(\mu) + Y_{\text{pert}}(\hat{s}) + Y_{\text{res}}(q^2). \quad (14)$$

The term  $C'_{b \rightarrow s\gamma}$  in Eq. (13) is the absorptive part of  $b \rightarrow s\gamma$  transition and was given in Ref. [55]

$$C'_{b \rightarrow s\gamma}(\mu) = i\alpha_s \left\{ \frac{2}{9}\eta^{14/23} \left[ \frac{x_t(x_t^2 - 5x_t - 2)}{8(x_t - 1)^3} + \frac{3x_t^2 \ln x_t}{4(x_t - 1)^4} - 0.1687 \right] - 0.03C_2(\mu) \right\}, \quad (15)$$

where  $x_t = m_t^2/m_W^2$  and  $\eta = \alpha_s(m_W)/\alpha_s(\mu)$ . The term  $Y_{\text{pert}}(\hat{s})$  in Eq. (14) defines the short distance perturbative part that involves the indirect contributions from the matrix element of the four quark operators  $\sum_{i=1}^{10} \langle \ell^+ \ell^- s | \mathcal{O}_i | b \rangle$  and lies at the place far away from  $c\bar{c}$  resonance regions. The term  $Y_{\text{pert}}(q^2)$  in Eq. (14) can be written in the following form [50, 56–59].

$$\begin{aligned} Y_{\text{pert}}(\hat{s}) = & 0.124\omega(\hat{s}) + g(\hat{m}_c, \hat{s})C_0 + \lambda_u [g(\hat{m}_c, \hat{s}) - g(\hat{m}_u, \hat{s})] (3C_1 + C_2) \\ & - \frac{1}{2}g(\hat{m}_d, \hat{s})(C_3 + 3C_4) - \frac{1}{2}g(\hat{m}_b, \hat{s})(4C_3 + 4C_4 + 3C_5 + C_6) \\ & + \frac{2}{9}(3C_3 + C_4 + 3C_5 + C_6), \end{aligned} \quad (16)$$

where  $C_0 = 3C_1 + C_2 + 3C_3 + C_4 + 3C_5 + C_6$ ,  $\hat{s} = q^2/m_b^2$ ,  $\hat{m}_q = m_q/m_b$ . In Eqs. (16), the function  $\omega(\hat{s})$  is the soft-gluon correction to the matrix element of operator  $\mathcal{O}_9$ , while the functions  $g(\hat{m}_q, \hat{s})$  is related to the basic fermion loop. The contributions from four-quark operators  $\mathcal{O}_1 - \mathcal{O}_6$  are usually combined with coefficient  $C_9$  into an "effective" one. One can find the explicit expressions of the function  $\omega(\hat{s})$  and  $g(\hat{m}_q, \hat{s})$  directly for example in Ref. [32] and references therein.

The term  $Y_{\text{res}}(q^2)$  in Eq. (14) describes the long distribution contribution to  $C_9^{\text{eff}}$ . But it can not be calculated from the first principle of QCD and may also introduce the double-counting problem with  $Y_{\text{pert}}(q^2)$ . For more details about such kinds of double-counting problem, one can see the discussions as given in Refs. [60, 61]. In this paper, we checked the possible effects on the theoretical predictions for those considered physical observables due to the inclusion of the term  $Y_{\text{res}}(q^2)$  as given in Ref. [50], and found that the resulted variations are less than 5% with or without the inclusion of  $Y_{\text{res}}(q^2)$ , which is much smaller than the general theoretical errors. According to the argument in Ref. [62], the term  $Y_{\text{res}}(q^2)$  is generally small. In order to avoid the possible double-counting problem we here simply drop the term  $Y_{\text{res}}(q^2)$  in our numerical evaluations.

### C. $B_s \rightarrow \phi$ transition form factors

For the vector meson  $\phi$  with polarization vector  $\epsilon^*$ , as usual, the relevant form factors for  $B_s \rightarrow \phi$  transitions are  $V(q^2)$  and  $A_{0,1,2}(q^2)$  of the vector and axial-vector currents, and  $T_{1,2,3}$  of the tensor currents. Between the form factors  $A_{0,1,2}(q^2)$  at the point  $q^2 = 0$ , there is an exact relation  $2m_\phi A_0(0) = (m_{B_s} + m_\phi)A_1(0) - (m_{B_s} - m_\phi)A_2(0)$  in order to avoid the kinematical singularity. Between the form factor  $T_{1,2}$ , there also exist a relation  $T_1(0) = T_2(0)$  in an algebraic manner which is implied by the identity  $\sigma^{\mu\nu}\gamma_5 = -\frac{i}{2}\epsilon^{\mu\nu\alpha\beta}\sigma_{\alpha\beta}$  with the  $\epsilon^{0123} = +1$  convention for the Levi-Civita tensor. Using the well-studied wave functions as given in Sec. II A, one can calculate all relevant form factors using the PQCD factorization approach as we did for example in Ref. [32].

One can find the expressions of the form factors from those as given in Ref. [32] for the case of  $B_s \rightarrow K^*$  transitions by simple replacements of the mass and the DAs between vector meson  $K^*$  and  $\phi$ . For the sake the reader, we also present all form factors explicitly in Appendix A.

### III. OBSERVABLES FOR $B_s \rightarrow \phi \ell^+ \ell^-$ DECAYS

In experimental analysis, the  $\bar{B}_s \rightarrow \phi \ell^+ \ell^-$  decay is treated as the four body differential decay distribution  $\bar{B}_s \rightarrow \phi(\rightarrow K^+ K^-) \ell^+ \ell^-$ , and has been described in terms of the four kinematic variables [10, 11, 13, 19]: the lepton invariant mass squared  $q^2$  and the three decay angles  $\vec{\Omega} = (\cos \theta_K, \cos \theta_\ell, \Phi)$ . The angle  $\theta_K$  is the angle between the direction of flight of  $K^+$  and  $B_s$  meson in the rest frame of  $\phi$ ,  $\theta_\ell$  is the angle made by  $\ell^-$  with respect to the  $B_s$  meson in the dilepton rest frame and  $\Phi$  is the azimuthal angle between the two planes formed by dilepton and  $K^+ K^-$ .

With the hadronic and leptonic amplitudes defined in Eq. (12), we write down the four fold differential distribution of four-body  $\bar{B}_s \rightarrow \phi(\rightarrow K^+ K^-) \ell^+ \ell^-$  decay [13, 49, 63, 64],

$$\frac{d^4 \Gamma}{dq^2 d\vec{\Omega}} = \frac{9}{32\pi} I(q^2, \vec{\Omega}), \quad d\vec{\Omega} = d \cos \theta_K d \cos \theta_\ell d\Phi, \quad (17)$$

where the functions  $I(q^2, \vec{\Omega})$  can be written in terms of a set of angular coefficients and trigonometric functions [63]:

$$\begin{aligned} I(q^2, \vec{\Omega}) &= \sum_i I_i(q^2) f_i(\vec{\Omega}) \\ &= I_{1s} \sin^2 \theta_K + I_{1c} \cos^2 \theta_K + (I_{2s} \sin^2 \theta_K + I_{2c} \cos^2 \theta_K) \cos 2\theta_\ell \\ &\quad + I_3 \sin^2 \theta_K \sin^2 \theta_\ell \cos 2\Phi + I_4 \sin 2\theta_K \sin 2\theta_\ell \cos \Phi \\ &\quad + I_5 \sin 2\theta_K \sin \theta_\ell \cos \Phi + I_{6s} \sin^2 \theta_K \cos \theta_\ell + I_7 \sin 2\theta_K \sin \theta_\ell \sin \Phi \\ &\quad + I_8 \sin 2\theta_K \sin 2\theta_\ell \sin \Phi + I_9 \sin^2 \theta_K \sin^2 \theta_\ell \sin 2\Phi. \end{aligned} \quad (18)$$

For the CP-conjugated mode  $B_s \rightarrow \phi(\rightarrow K^- K^+) \ell^+ \ell^-$ , the corresponding expression of the angular decay distribution is

$$\frac{d^4 \bar{\Gamma}}{dq^2 d\vec{\Omega}} = \frac{9}{32\pi} \bar{I}(q^2, \vec{\Omega}), \quad (19)$$

where the function  $\bar{I}(q^2, \vec{\Omega})$  is obtained from  $I(q^2, \vec{\Omega})$  in Eq. (18) by making the complex conjugation for all weak phases in  $I_i$  [63], and numerically by the following substitution:

$$I_{1(c,s),2(c,s),3,4,7} \rightarrow \bar{I}_{1(c,s),2(c,s),3,4,7}, \quad I_{5,6s,8,9} \rightarrow -\bar{I}_{5,6s,8,9}. \quad (20)$$

The minus sign in Eq. (20) is a result of the convention that, under the previous definitions of three angles  $(\theta_K, \theta_\ell, \Phi)$ , a CP transformation interchanges the lepton and anti-lepton, i.e., leading to the transformation  $\theta_\ell \rightarrow \theta_\ell - \pi$  and  $\Phi \rightarrow -\Phi$ .

The angular coefficients  $I_i$ , which are functions of  $q^2$  only, are usually expressed in terms of the transverse amplitudes [8, 13]. In the limit of massless leptons, there are six such complex amplitudes:  $\mathcal{A}_0^{L,R}$ ,  $\mathcal{A}_\parallel^{L,R}$  and  $\mathcal{A}_\perp^{L,R}$ , where  $L$  and  $R$  refer to the chirality of the leptonic current. For the massive case, an additional complex amplitude  $\mathcal{A}_t$  is required, where the timelike component of the virtual gauge boson (which can later decay into dilepton) couple to an axial-vector current.

In Table I, we summarize the treatment of the angular distribution by decomposition of the angular coefficients  $I_i(q^2)$  into seven transverse amplitude  $\mathcal{A}_{\perp,\parallel,0}^{L,R}$  and  $\mathcal{A}_t$  as well as the corresponding trigonometric factor  $f_i(\vec{\Omega})$ . Here we will not consider scalar contribution to

facilitate the comparison with Ref. [32]. Notice that the distribution including lepton masses (but neglecting scalar  $I_{6c} = 0$ ) contains eleven  $I_i$  where only 10 of them are independent [8, 65]. In the limit of massless leptons, it is easy to obtain the relations  $I_{1s} = 3I_{2s}$  and  $I_{1c} = -I_{2c}$  [63].

TABLE I: The explicit expressions of the angular coefficients  $I_i(q^2)$  and  $f_i(\vec{\Omega})$  appeared in Eq. (18).

$i$	$I_i(q^2)$	$f_i(\vec{\Omega})$
1s	$(\frac{3}{4} - \hat{m}_\ell^2) [ \mathcal{A}_\parallel^L ^2 +  \mathcal{A}_\perp^L ^2 +  \mathcal{A}_\parallel^R ^2 +  \mathcal{A}_\perp^R ^2] + 4\hat{m}_\ell^2 \text{Re} [\mathcal{A}_\perp^L \mathcal{A}_\perp^{R*} + \mathcal{A}_\parallel^L \mathcal{A}_\parallel^{R*}]$	$\sin^2 \theta_K$
1c	$ \mathcal{A}_0^L ^2 +  \mathcal{A}_0^R ^2 + 4\hat{m}_\ell^2 [ \mathcal{A}_t ^2 + 2\text{Re}[\mathcal{A}_0^L \mathcal{A}_0^{R*}]]$	$\cos^2 \theta_K$
2s	$\frac{1}{4}\beta_\ell^2 [ \mathcal{A}_\parallel^L ^2 +  \mathcal{A}_\perp^L ^2 +  \mathcal{A}_\parallel^R ^2 +  \mathcal{A}_\perp^R ^2]$	$\sin^2 \theta_K \cos 2\theta_\ell$
2c	$-\beta_\ell^2 [ \mathcal{A}_0^L ^2 +  \mathcal{A}_0^R ^2]$	$\cos^2 \theta_K \cos 2\theta_\ell$
3	$\frac{1}{2}\beta_\ell^2 [ \mathcal{A}_\perp^L ^2 -  \mathcal{A}_\parallel^L ^2 +  \mathcal{A}_\perp^R ^2 -  \mathcal{A}_\parallel^R ^2]$	$\sin^2 \theta_K \sin^2 \theta_\ell \cos 2\Phi$
4	$\sqrt{\frac{1}{2}}\beta_\ell^2 \text{Re}(\mathcal{A}_0^L \mathcal{A}_\parallel^{L*} + \mathcal{A}_0^R \mathcal{A}_\parallel^{R*})$	$\sin 2\theta_K \sin 2\theta_\ell \cos \Phi$
5	$\sqrt{2}\beta_\ell \text{Re}(\mathcal{A}_0^L \mathcal{A}_\perp^{L*} - \mathcal{A}_0^R \mathcal{A}_\perp^{R*})$	$\sin 2\theta_K \sin \theta_\ell \cos \Phi$
6s	$2\beta_\ell \text{Re}(\mathcal{A}_\parallel^L \mathcal{A}_\perp^{L*} - \mathcal{A}_\parallel^R \mathcal{A}_\perp^{R*})$	$\sin^2 \theta_K \cos \theta_\ell$
7	$\sqrt{2}\beta_\ell \text{Im}(\mathcal{A}_0^L \mathcal{A}_\parallel^{L*} - \mathcal{A}_0^R \mathcal{A}_\parallel^{R*})$	$\sin 2\theta_K \sin \theta_\ell \sin \Phi$
8	$\sqrt{\frac{1}{2}}\beta_\ell^2 \text{Im}(\mathcal{A}_0^L \mathcal{A}_\perp^{L*} + \mathcal{A}_0^R \mathcal{A}_\perp^{R*})$	$\sin 2\theta_K \sin 2\theta_\ell \sin \Phi$
9	$\beta_\ell^2 \text{Im}(\mathcal{A}_\parallel^{L*} \mathcal{A}_\perp^L + \mathcal{A}_\parallel^{R*} \mathcal{A}_\perp^R)$	$\sin^2 \theta_K \sin^2 \theta_\ell \sin 2\Phi$

The seven transverse amplitudes  $\mathcal{A}_0^{L,R}$ ,  $\mathcal{A}_\parallel^{L,R}$ ,  $\mathcal{A}_\perp^{L,R}$  and  $\mathcal{A}_t$  of  $B_s \rightarrow \phi \ell^+ \ell^-$  decay, in turn, can be parameterized by means of the relevant form factors [63, 66]:

$$\mathcal{A}_\perp^{L,R} = -N_\ell \sqrt{2N_\phi} \sqrt{\lambda} \left[ (C_9^{\text{eff}} \mp C_{10}) \frac{V(q^2)}{m_{B_s} + m_\phi} + 2\hat{m}_b C_7^{\text{eff}} T_1(q^2) \right], \quad (21)$$

$$\mathcal{A}_\parallel^{L,R} = N_\ell \sqrt{2N_\phi} \left[ (C_9^{\text{eff}} \mp C_{10})(m_{B_s} + m_\phi) A_1(q^2) + 2\hat{m}_b C_7^{\text{eff}} (m_{B_s}^2 - m_\phi^2) T_2(q^2) \right], \quad (22)$$

$$\begin{aligned} \mathcal{A}_0^{L,R} = & \frac{N_\ell \sqrt{N_\phi}}{2m_\phi \sqrt{q^2}} \left\{ (C_9^{\text{eff}} \mp C_{10}) \left[ (m_{B_s}^2 - m_\phi^2 - q^2)(m_{B_s} + m_\phi) A_1(q^2) - \frac{\lambda}{m_{B_s} + m_\phi} A_2(q^2) \right] \right. \\ & \left. + 2m_b C_7^{\text{eff}} \left[ (m_{B_s}^2 + 3m_\phi^2 - q^2) T_2(q^2) - \frac{\lambda}{m_{B_s}^2 - m_\phi^2} T_3(q^2) \right] \right\}, \end{aligned} \quad (23)$$

$$\mathcal{A}_t = 2N_\ell \sqrt{N_\phi} \frac{\sqrt{\lambda}}{\sqrt{q^2}} C_{10} A_0(q^2), \quad (24)$$

where  $\lambda = (m_{B_s}^2 - m_\phi^2 - q^2)^2 - 4m_\phi^2 q^2$ ,  $\hat{m}_b = m_b/q^2$  and the normalization constants are given as:

$$N_\ell = \frac{i\alpha_{em} G_F}{4\sqrt{2}\pi} V_{tb} V_{ts}^*, \quad N_\phi = \frac{8\sqrt{\lambda} q^2}{3 \times 256\pi^3 m_{B_s}^3} \sqrt{1 - \frac{4m_\ell^2}{q^2}} \mathcal{B}(\phi \rightarrow K^+ K^-). \quad (25)$$

In numerical calculations, we take  $\mathcal{B}(\phi \rightarrow K^+ K^-) = 0.492$  from PDG 2018 [67]. It is easy to see that the narrow width approximation works well in the case of  $\phi$  meson since  $\Gamma_\phi/m_\phi = 4.17 \times 10^{-3} \sim 0$ .

Analogous to Ref. [63], to separate CP-conserving and CP-violating effects, one can define the CP averaged angular coefficients  $S_i$  and CP asymmetry angular coefficients  $A_i$  normalized by the differential (CP-averaged) decay rate to reduce the theoretical uncertainties,

$$S_i = \frac{I_i + \bar{I}_i}{d(\Gamma + \bar{\Gamma})/dq^2}, \quad A_i = \frac{I_i - \bar{I}_i}{d(\Gamma + \bar{\Gamma})/dq^2}, \quad (26)$$

where  $I_i$  and  $\bar{I}_i$  have been defined in Eqs. (18,19,20) and Table I, and the differential decay rate reads (analogously for  $\bar{\Gamma}$ ),

$$\frac{d\Gamma}{dq^2} = \frac{1}{4} (3I_{1c} + 6I_{1s} - I_{2c} - 2I_{2s}). \quad (27)$$

Based on the definition of  $S_i$ , one can find the relation  $3S_{1c} + 6S_{1s} - S_{2c} - 2S_{2s} = 4$ .

Consequently, all established observables can be expressed in terms of  $S_i$  and  $A_i$ :

(1) the CP asymmetry

$$A_{\text{CP}}(q^2) = \frac{d\Gamma/dq^2 - d\bar{\Gamma}/dq^2}{d\Gamma/dq^2 + d\bar{\Gamma}/dq^2} = \frac{1}{4} (3A_{1c} + 6A_{1s} - A_{2c} - 2A_{2s}). \quad (28)$$

(2) The lepton forward-backward (CP) asymmetry:

$$A_{\text{FB}}(q^2) = \frac{\left[ \int_0^1 - \int_{-1}^0 \right] d \cos \theta_\ell \frac{d^2(\Gamma - \bar{\Gamma})}{dq^2 d \cos \theta_\ell}}{d(\Gamma + \bar{\Gamma})/dq^2} = \frac{3}{4} S_{6s}, \quad (29)$$

$$A_{\text{FB}}^{\text{CP}}(q^2) = \frac{\left[ \int_0^1 - \int_{-1}^0 \right] d \cos \theta_\ell \frac{d^2(\Gamma + \bar{\Gamma})}{dq^2 d \cos \theta_\ell}}{d(\Gamma + \bar{\Gamma})/dq^2} = \frac{3}{4} A_{6s}. \quad (30)$$

(3) The  $\phi$  polarization fractions:

$$F_L(q^2) = \frac{1}{4} (3S_{1c} - S_{2c}), \quad F_T(q^2) = \frac{1}{2} (3S_{1s} - S_{2s}). \quad (31)$$

In the massless limit, since the CP-averaged observable  $S_{1(c,s),2(c,s)}$  obey the relations  $S_{1s} = 3S_{2s}$  and  $S_{1c} = -S_{2c}$ , the definitions of the polarization fractions can be simplified directly as:

$$F_L(q^2) = S_{1c} = -S_{2c}, \quad F_T(q^2) = \frac{4}{3} S_{1s} = 4S_{2s}. \quad (32)$$

(4) The clean (no S-wave pollution) observables  $P_{1,2,3}$  and  $P'_{4,5,6}$  in the natural basis can be defined in terms of the coefficients  $S_i$  through the following relations [64, 68, 69]:

$$P_1 = \frac{S_3}{2S_{2s}}, \quad P_2 = \beta_\ell \frac{S_{6s}}{8S_{2s}}, \quad P_3 = -\frac{S_9}{4S_{2s}}, \quad (33)$$

$$P'_4 = \frac{S_4}{\sqrt{S_{1c}S_{2s}}}, \quad P'_5 = \frac{\beta_\ell S_5}{2\sqrt{S_{1c}S_{2s}}}, \quad P'_6 = -\frac{\beta_\ell S_7}{2\sqrt{S_{1c}S_{2s}}}, \quad P'_8 = -\frac{S_8}{\sqrt{S_{1c}S_{2s}}}, \quad (34)$$

where  $\beta_\ell = \sqrt{1 - 4m_\ell^2/q^2}$ .

- (5) In the massless limit of leptons, the optimised observables  $P_i^{(\prime)}$  [8] can be transformed as the following form:

$$P_1 = \frac{2S_3}{F_T}, \quad P_2 = \frac{S_{6s}}{2F_T}, \quad P_3 = \frac{-S_9}{F_T}, \quad (35)$$

$$P'_4 = \frac{2S_4}{\sqrt{F_L(1-F_L)}}, \quad P'_5 = \frac{S_5}{\sqrt{F_L(1-F_L)}},$$

$$P'_6 = -\frac{S_7}{\sqrt{F_L(1-F_L)}}, \quad P'_8 = -\frac{2S_8}{\sqrt{F_L(1-F_L)}}. \quad (36)$$

One should know that our definitions of the CP averaged angular coefficients  $S_i$ , the CP asymmetry angular coefficients  $A_i$  and the clean observable  $P_{1,2,3}$  and  $P'_{4,5,6}$  differ from those adopted by the LHCb collaboration. To be specific, the reasons are the following:

- (1) Our conventions for the angles to define the  $B_s \rightarrow \phi \ell^+ \ell^-$  kinematics are identical to the Ref. [63] but different from the LHCb choices [13, 31]. The corresponding relations are the following :

$$\theta_K^{\text{LHCb}} = \theta_K, \quad \theta_\ell^{\text{LHCb}} = \pi - \theta_\ell, \quad \Phi^{\text{LHCb}} = -\Phi. \quad (37)$$

Some angular coefficients  $I_i$ ,  $S_i$  and  $A_i$ , consequently, will have different signs:

$$I_{4,6,7,9}^{\text{LHCb}} = -I_{4,6s,7,9}, \quad S_{4,6,7,9}^{\text{LHCb}} = -S_{4,6s,7,9}, \quad A_{4,6,7,9}^{\text{LHCb}} = -A_{4,6s,7,9}. \quad (38)$$

Other remaining coefficients  $I_i$  ( $S_i$  and  $A_i$ ), however, have the same sign in both conventions.

- (2) Our definitions of the clean observables  $P_{1,2,3}$  and  $P'_{4,5,6,8}$  in Eq. (34) in terms of  $S_i$  may be different from those defined and used by the LHCb Collaboration for example in Ref. [13]. The resultant differences of the sign and normalization are of the following:

$$P_1^{\text{LHCb}} = P_1, \quad P_{2,3}^{\text{LHCb}} = -P_{2,3}, \quad P_{4,8}^{\text{LHCb}} = -\frac{1}{2}P'_{4,8}, \quad P_{5,6}^{\text{LHCb}} = P'_{5,6}. \quad (39)$$

For more details about the angular conventions of the angular observables of the semileptonic decays  $B_{(s)} \rightarrow V l^+ l^-$ , one can see Ref. [70].

#### IV. NUMERICAL RESULTS AND DISCUSSIONS

In the numerical calculations we use the following input parameters (here masses and decay constants are in units of GeV) [67]:

$$\Lambda_{\overline{\text{MS}}}^{f=4} = 0.250, \quad \tau_{B_s^0} = 1.509\text{ps}, \quad m_b = 4.8, \quad m_W = 80.38, \quad m_\phi = 1.019$$

$$m_{B_s} = 5.367, \quad m_e = 0.000511, \quad m_\mu = 0.105, \quad m_\tau = 1.777,$$

$$f_{B_s} = 0.23, \quad f_\phi = 0.231 \pm 0.004, \quad f_\phi^T = 0.200 \pm 0.01,$$

$$a_{2\phi}^\parallel = 0.18 \pm 0.08, \quad a_{2\phi}^\perp = 0.14 \pm 0.07. \quad (40)$$

For the CKM matrix elements and angles, we adopt the independently measured parametrization with the updated parameters as [67]:

$$\begin{aligned} V_{tb} &= 1.019 \pm 0.025, & V_{us} &= 0.2243 \pm 0.0005, \\ V_{ts} &= |V_{ts}|e^{-i\beta_s}, & |V_{ts}| &= (39.4 \pm 2.3) \times 10^{-3}, & 2\beta_s &= 0.021 \pm 0.031, \\ V_{ub} &= |V_{ub}|e^{-i\gamma}, & |V_{ub}| &= (3.94 \pm 0.36) \times 10^{-3}, & \gamma &= (73.5^{+4.2}_{-5.1})^\circ. \end{aligned} \quad (41)$$

### A. The form factors extrapolations

For the considered semileptonic decays, the differential decay rates and other physical observables strongly rely on the value and the shape of the relevant form factors  $V(q^2)$ ,  $A_{0,1,2}(q^2)$  and  $T_{1,2,3}(q^2)$  for  $B_s \rightarrow \phi \ell^+ \ell^-$  decays. These form factors have been calculated in rather different theories or models [23, 33–35, 42]. Since the PQCD predictions for the considered form factors are valid only at the large hadronic recoil (low- $q^2$ ) region, we usually calculate explicitly the values of the relevant form factors at the low- $q^2$  region, say  $0 \leq q^2 \leq m_\tau^2$ , and then make an extrapolation for all relevant form factors from the low- $q^2$  towards the high- $q^2$  region by using the pole model parametrization [71, 72] or other different methods.

In Refs. [73–75], we developed a new method: the so-called “PQCD+Lattice” approach. Here we still use the PQCD approach to evaluate the form factors at the low  $q^2$  region, but take those currently available lattice QCD results for the relevant form factors at the high- $q^2$  region as the lattice QCD input to improve the extrapolation of the form factors up to  $q_{max}^2$ . In Refs. [74, 75], we used the Bourrely-Caprini-Lellouch (BCL) parametrization method [76, 77] instead of the traditional pole model parametrization.

In Table II, for the  $B_s \rightarrow \phi$  transition form factors ( $V(q^2), A_{0,1}(q^2), T_{1,2}(q^2)$ ), we quote directly the values of the lattice QCD results at three reference points of the high  $q^2$  region, say  $q^2 = 12, 16 \text{ GeV}^2$  and  $q_{max}^2 = (m_{B_s} - m_\phi)^2 \approx 18.9 \text{ GeV}^2$ , as listed in Table XXXI of Ref. [78]. In Ref. [78], the authors defined the helicity form factors  $A_{12}(q^2)$  and  $T_{23}(q^2)$  from the ordinary form factors  $A_{1,2}(q^2)$  and  $T_{2,3}(q^2)$ :

$$\begin{aligned} A_{12}(q^2) &= \frac{(m_{B_s} + m_\phi)^2(m_{B_s}^2 - m_\phi^2 - q^2)A_1(q^2) - \lambda A_2(q^2)}{16m_{B_s}m_\phi^2(m_{B_s} + m_\phi)}, \\ T_{23}(q^2) &= \frac{m_{B_s} + m_\phi}{8m_{B_s}m_\phi^2} \left[ (m_{B_s}^2 + 3m_\phi^2 - q^2)T_2(q^2) - \frac{\lambda T_3(q^2)}{m_{B_s}^2 - m_\phi^2} \right], \end{aligned} \quad (42)$$

where the kinematic variable  $\lambda = (t_+ - q^2)(t_- - q^2)$  with  $t_\pm = (m_{B_s} \pm m_\phi)^2$ . From above two equations and the numerical values of  $(A_1(q^2), T_2(q^2), A_{12}(q^2), T_{23}(q^2))$  as given in Table XXXI of Ref. [78], we can find the corresponding lattice QCD results of  $A_2(q^2)$  and  $T_3(q^2)$  at the two points  $q^2 = (12, 16) \text{ GeV}^2$  by direct numerical calculations. Since when  $q^2 \rightarrow q_{max}^2$ , the parameter  $\lambda(q_{max}^2)$  in Eq. (42) is also approaching zero simultaneously. One therefore can not determine  $A_2(q_{max}^2)$  and  $T_3(q_{max}^2)$  reliably from the values of  $(A_{12}(q_{max}^2)$  and  $T_{23}(q_{max}^2))$  as given in Ref. [78]. For the sake of the reader, we list in Table II the lattice QCD results of all relevant form factors at three reference points of high  $q^2$  region.

In this work, we will use both the PQCD factorization approach and the “PQCD+Lattice” approach to evaluate all relevant form factors over the whole range of  $q^2$ .

TABLE II: The values for the lattice QCD results of the relevant  $B_s \rightarrow \phi$  transition form factors at three reference points of  $q^2$ :  $q^2 = 12, 16 \text{ GeV}^2$  and  $q_{max}^2 = (m_{B_s} - m_\phi)^2 \approx 18.9 \text{ GeV}^2$  [78].

$q^2$	$V(q^2)$	$A_0(q^2)$	$A_1(q^2)$	$A_2(q^2)$	$T_1(q^2)$	$T_2(q^2)$	$T_3(q^2)$
12	0.77(6)	0.90(6)	0.44(3)	0.48(4)	0.69(4)	0.45(3)	0.46(4)
16	1.19(7)	1.32(7)	0.52(3)	0.54(4)	0.99(5)	0.53(3)	0.70(5)
18.9	1.74(10)	1.85(10)	0.62(3)	—	1.36(8)	0.62(3)	—

- (1) In the PQCD approach, we use the definitions and formulae to calculate the values of all relevant form factors  $V(q^2)$ ,  $A_{0,1,2}(q^2)$  and  $T_{1,2,3}(q^2)$  in the low  $q^2$  region:  $0 \leq q^2 \leq m_\tau^2$ . We then make the extrapolation for these form factors to the large  $q^2$  region up to  $q_{max}^2$  by using the selected parametrization method.
- (2) In the “PQCD+Lattice” approach, we take the lattice QCD results for the form factors at some large  $q^2$  points as input and then make a combined fit to the PQCD and the lattice QCD results at the low and high  $q^2$  region.
- (3) For both approaches, we always use the model-independent  $z$ -series parametrization, which is based on a rapidly converging series in the parameter  $z$ , as in Refs. [23, 49] to make the extrapolation. The entire cut  $q^2$ -plane will be mapped onto the unit disc  $|z(q^2)| \leq 1$  under the conformal transformation as [79]

$$z(q^2) = \frac{\sqrt{t_+ - q^2} - \sqrt{t_+ - t_0}}{\sqrt{t_+ - q^2} + \sqrt{t_+ - t_0}} \quad (43)$$

where  $t_\pm = (m_{B_s} \pm m_\phi)^2$  and  $0 \leq t_0 < t_-$  is a auxiliary parameter which can be optimised to reduce the maximum value of  $|z(q^2)|$  in the physical range of the form factors and will be taken in the same way as in Ref. [80]:  $t_0 = t_+(1 - \sqrt{1 - t_-/t_+})$ . The form factors are finally parameterized in the BCL version of the  $z$ -series expansion [76]

$$F_{B_s \rightarrow \phi}^i(q^2) = \frac{F_{B_s \rightarrow \phi}^i(0)}{1 - q^2/m_{i,\text{pole}}^2} \left\{ 1 + \sum_{k=1}^N b_k^i [z(q^2, t_0)^k - z(0, t_0)^k] \right\}. \quad (44)$$

The input values of the various  $\bar{s}b$ -resonance masses with different quantum numbers  $J^P$  from PDG-2018 [67] are summarized in Table III. With the optimised value for  $t_0$ , the form factors can be well described by Eq.(44) which is truncated at  $N = 1$  for the purpose of fitting the coefficients  $b_k^i$  practically. The further discussions on the systematic uncertainties due to the dependence of truncation schemes and on the implementation of the strong unitary constraints can be seen in Refs. [80, 81].

- (4) In Fig. 1, we show the theoretical predictions of the form factors  $V(q^2), A_{0,1,2}(q^2)$  and  $T_{1,2,3}(q^2)$  for  $B_s \rightarrow \phi$  transition using the PQCD (red curves) and “PQCD+Lattice” (blue curves) approach with an extrapolation to the entire kinematical region by applying the  $z$ -series parameterizations. The red and blue shaded band represent the theory uncertainties in two approaches. The black error bars in low- $q^2$  and the high- $q^2$  region are the PQCD results and the lattice QCD inputs, respectively.

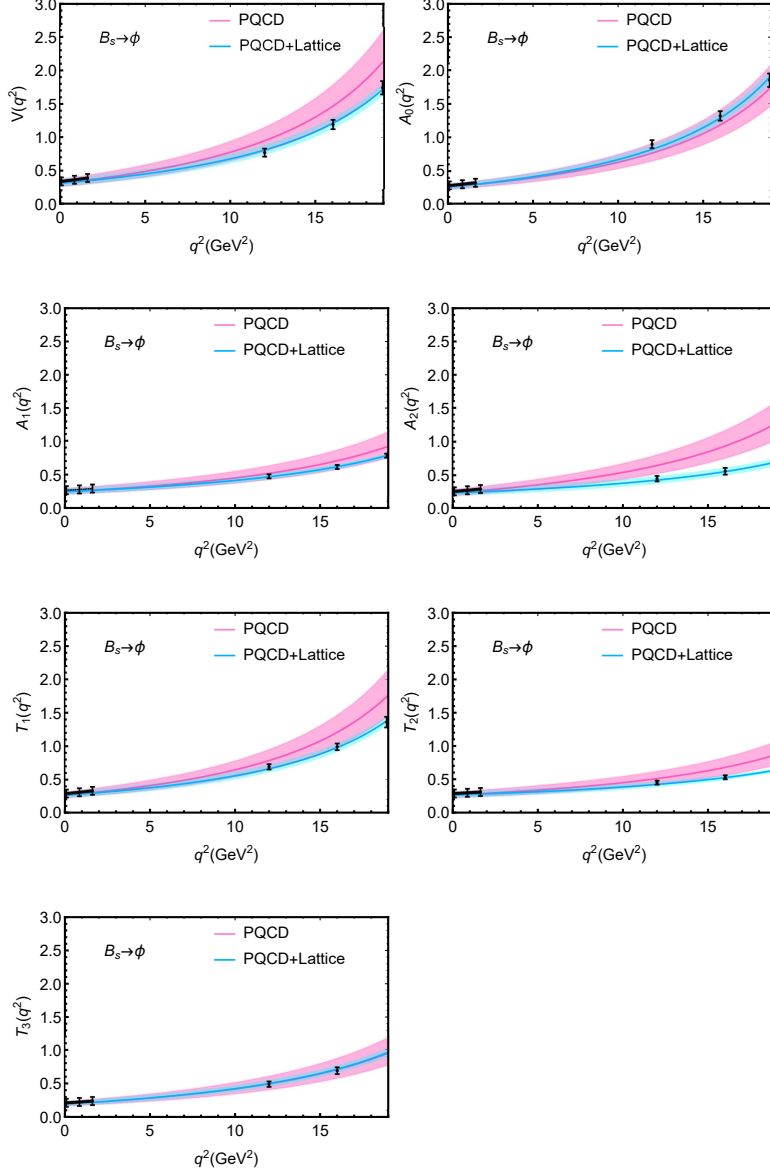


FIG. 1: Theoretical predictions of the relevant form factors for  $B_s \rightarrow \phi$  transition in the PQCD (red curves) and “PQCD+Lattice” (blue curves) approach with an extrapolation to the entire kinematical region by applying the  $z$ -series parameterizations. The red (blue) shaded band represents the theory uncertainties. The lattice data points with error in high- $q^2$  region can be found in Table II.

In Table IV, as a comparison, we show the central values of all relevant form factors in this work and other theoretical predictions as given in Refs. [20, 21, 40, 42, 82–88] at the scale  $q^2 = 0$ . There exist always some differences even among the authors using the same approach. Taking the calculations based on the LCSR method as an example, the authors of Ref. [23] introduced the hadronic input parameters, Ball and Zwicky considered the one-loop radiative corrections [20], Yilmaz included the radiative and higher twist corrections and SU(3) breaking effects [83]. In Fig. 1, we show the PQCD and “PQCD+Lattice” predictions for the form factors  $V(q^2)$ ,  $A_{0,1,2}(q^2)$  and  $T_{1,2,3}(q^2)$  in the whole range of  $0 \leq q^2 \leq q_{max}^2$ , where

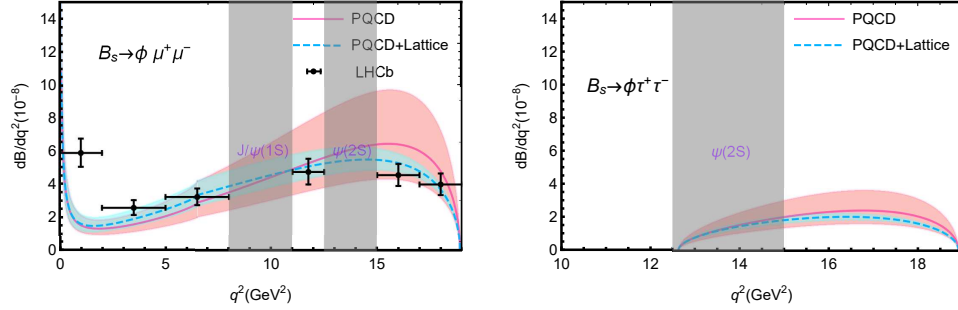


FIG. 2: Theoretical predictions for the  $q^2$ -dependence of differential branching fraction  $d\mathcal{B}/dq^2$  for the semileptonic decays  $B_s \rightarrow \phi \ell^+ \ell^-$  with  $\ell = (\mu, \tau)$  in the PQCD (red band) and “PQCD+Lattice” (blue band) approach, respectively. The crosses represents the LHCb measurements [31]. The vertical grey blocks are the experimental veto regions.

TABLE III: Masses of the  $\bar{s}b$ -resonance with different quantum numbers  $J^P$  entering the  $z$ -series expansions Eq. (44) for the parameterisation of  $B_s \rightarrow \phi$  form factors  $F_i$  corresponding to  $b \rightarrow s$  transition at quark level [23].

$F_i^{B_s \rightarrow \phi}(q^2)$	$\bar{s}b(J^P)$	$m_{i,\text{pole}}(\text{GeV})$
$A_0(q^2)$	$B_s(0^-)$	5.366
$V(q^2), T_1(q^2)$	$B_s^*(1^-)$	5.415
$A_{1,2}(q^2), T_{2,3}(q^2)$	$B_{s1}(1^+)$	5.829

the theory uncertainties are obtained by adding all the separate uncertainties in quadrature. Although there are some real differences between the theoretical predictions obtained by employing different approaches or models, they are generally consistent with each other within the still large theoretical uncertainties.

## B. Observables for $B_s \rightarrow \phi \ell^+ \ell^-$

We now proceed to explore the phenomenological aspects of the cascade decays  $B_s \rightarrow \phi(\rightarrow K^- K^+) \ell^+ \ell^-$ , which allows us to define and compute a number of physical observables and compare them with those measured by experiments. We first compare our results for the branching ratios and angular observables with the experimental data reported by the LHCb Collaboration[31]. As studied systematically in last section, the physical observables accessible in the semileptonic decays  $B_s \rightarrow \phi \ell^+ \ell^-$  [31] are the CP averaged differential branching fraction  $d\mathcal{B}/dq^2$ , the CP-averaged  $\phi$  meson longitudinal polarization fraction  $F_L$ , the forward-backward asymmetry  $\mathcal{A}_{FB}$ , the angular coefficients  $S_i$  and  $A_i$ , and the optimized observables  $P_i$  and  $P'_j$  [25]. The CP asymmetry angular coefficients  $A_{5,6,8,9}$  in the SM are induced by the weak phase from the CKM matrix. For the  $b \rightarrow s$  transition, the CP asymmetries proportional to  $\text{Im}(V_{ub}V_{us}^*/V_{tb}V_{ts}^*)$ , which is of order  $10^{-2}$  [19] as measured by the LHCb Collaboration (see Table 3 in Ref. [31]), but the statistical uncertainties are still large. For these reasons, we will focus on the CP averaged quantities when taking the binned observables into consideration.

We begin with the branching ratios of the decays  $B_s \rightarrow \phi \ell^+ \ell^-$ . From the differential

TABLE IV: The theoretical predictions for the central values of the form factors of the  $B_s \rightarrow \phi$  transitions at  $q^2 = 0$  obtained by using rather different theories or models.

	$V(0)$	$A_0(0)$	$A_1(0)$	$A_2(0)$	$T_{1,2}(0)$	$T_3(0)$
This work	0.31	0.26	0.25	0.24	0.26	0.20
PQCD[42]	0.25	0.30	0.19	—	—	—
PQCD[82]	0.26	0.31	0.18	0.12	0.23	0.19
LCSR[23]	0.387	0.389	0.296	—	0.309	—
LCSR[20]	0.434	0.474	0.311	0.234	0.349	0.175
LCSR[83]	0.433	0.382	0.296	0.255	0.348	0.254
QCDSR[84]	0.45	0.30	0.32	0.30	0.33	0.22
RDA[85]	0.44	0.42	0.34	0.31	0.38	0.26
RQM[86]	0.406	0.322	0.320	0.318	0.275	0.133
SCET[87]	0.329	0.279	0.232	0.210	0.276	0.170
HQFT[21]	0.339	0.269	0.271	0.212	0.299	0.191
SQEH[88]	0.259	0.311	0.194	—	—	—
CQM[17]	0.31	0.28	0.27	0.27	0.27	0.18

TABLE V: Theoretical predictions for the total branching fractions  $\mathcal{B}(B_s \rightarrow \phi \ell^+ \ell^-)$  ( in units of  $10^{-7}$  ) in the PQCD (the first row) and “PQCD+Lattice” (the second row) approaches. As a comparison, we also list the LHCb measured value for muon channel [31] and the QCDSR predictions for all three channels [84].

BFs	PQCD / “PQCD+Lattice”	QCDSR [84]	LHCb [31]
$\mathcal{B}(B_s \rightarrow \phi e^+ e^-)$	$8.55^{+4.02}_{-2.69}(\text{FFs}) \pm 0.15(\mu) \pm 0.42(V_{\text{tb}}) \pm 0.65(V_{\text{ts}})$	$7.12 \pm 1.40$	$7.97^{+0.81}_{-0.80}$
	$8.24^{+2.03}_{-1.53}(\text{FFs}) \pm 0.14(\mu) \pm 0.41(V_{\text{tb}}) \pm 0.63(V_{\text{ts}})$		
$\mathcal{B}(B_s \rightarrow \phi \mu^+ \mu^-)$	$7.07^{+3.37}_{-2.25}(\text{FFs}) \pm 0.12(\mu) \pm 0.38(V_{\text{tb}}) \pm 0.53(V_{\text{ts}})$	$7.06 \pm 1.59$	
	$6.76^{+1.39}_{-1.09}(\text{FFs}) \pm 0.11(\mu) \pm 0.33(V_{\text{tb}}) \pm 0.52(V_{\text{ts}})$		
$\mathcal{B}(B_s \rightarrow \phi \tau^+ \tau^-)$	$0.81^{+0.42}_{-0.27}(\text{FFs}) \pm 0.02(\mu) \pm 0.04(V_{\text{tb}}) \pm 0.06(V_{\text{ts}})$	$0.35 \pm 0.17$	
	$0.68^{+0.06}_{-0.06}(\text{FFs}) \pm 0.02(\mu) \pm 0.03(V_{\text{tb}}) \pm 0.05(V_{\text{ts}})$		

decay rates as defined in Eq. (27), it is straightforward to make the integration over the range of  $4m_\ell^2 \leq q^2 \leq (m_{B_s} - m_\phi)^2$ . In order to be consistent with the choices made by LHCb Collaboration in their data analysis, we here also cut off the regions of dilepton-mass squared around the charmonium resonances  $J/\psi(1S)$  and  $\psi(2S)$ : i.e.,  $8.0 < q^2 < 11.0 \text{ GeV}^2$  and  $12.5 < q^2 < 15.0 \text{ GeV}^2$  for  $\ell = (e, \mu, \tau)$  cases. We display the PQCD and “PQCD+Lattice” predictions for the differential branching ratios  $d\mathcal{B}/dq^2$  in Fig. 2 for the cases of  $\ell = (\mu, \tau)$ , including currently available LHCb results in six bins of  $q^2$  [31] indicated by the crosses for  $B_s \rightarrow \phi \mu^+ \mu^-$ . From Fig. 2 one can see that both PQCD and “PQCD+Lattice” predictions for the differential branching ratios do agree well with the LHCb results within the still large errors. Since the theoretical prediction for the differential branching ratio of the electron mode is almost identical with the one of the muon, we do not draw the figure of  $d\mathcal{B}(B_s \rightarrow \phi e^+ e^-)/dq^2$  in Fig. 2.

In Table V we present the theoretical predictions of the total branching fractions for

$B_s \rightarrow \phi \ell^+ \ell^-$  with  $\ell = (e, \mu, \tau)$  obtained by the integration over the six  $q^2$  bins using the PQCD ( the first row) and “PQCD+Lattice” approach ( the second row), respectively. The major theoretical errors from different sources, such as the form factors (FFs), the scale  $\mu$ , the CKM matrix element  $V_{tb}$  and  $V_{ts}$ , are also listed. As in Ref. [31], a correction factor  $f_{veto} = 1.52$  is applied to account for the contribution in the veto  $q^2$  bins for  $\ell = (e, \mu)$  cases. As a comparison, we also show the LHCb result  $\mathcal{B}(B_s \rightarrow \phi \mu^+ \mu^-) = (7.97_{-0.80}^{+0.81}) \times 10^{-7}$  and the QCDSR predictions  $\mathcal{B}(B_s \rightarrow \phi \ell^+ \ell^-)$  for all three decay modes [84]. For  $B_s \rightarrow \phi \mu^+ \mu^-$  decay, for instance, the theoretical predictions and the LHCb measurement [31] (in unit of  $10^{-7}$ ) are the following:

$$\mathcal{B}(B_s \rightarrow \phi \mu^+ \mu^-) = \begin{cases} 7.07_{-2.34}^{+3.43}, & \text{in PQCD,} \\ 6.76_{-1.25}^{+1.52}, & \text{in PQCD + Lattice,} \\ 7.06_{-1.59}^{+1.59}, & \text{in QCDSR [84],} \\ 7.97_{-0.80}^{+0.81}, & \text{LHCb [31].} \end{cases} \quad (45)$$

From the numerical results in above equation and Table V, one can see that

- (1) The PQCD and “PQCD+Lattice” predictions for the branching ratio  $\mathcal{B}(B_s \rightarrow \phi \ell^+ \ell^-)$  with  $\ell = (e, \mu, \tau)$  do agree well with each other within the errors, while the “PQCD+Lattice” predictions of  $\mathcal{B}(B_s \rightarrow \phi \ell^+ \ell^-)$  have smaller errors than those of the PQCD predictions.
- (2) Both PQCD and “PQCD+Lattice” predictions of  $\mathcal{B}(B_s \rightarrow \phi \mu^+ \mu^-)$  do agree well with currently available LHCb measured value [31] within errors. For the electron and tau mode, however, we have to wait for the future experimental measurements.
- (3) For all three decay modes, our theoretical predictions of the branching ratios do agree well with the theoretical predictions obtained from the QCD sum rule [84].

Since the large theoretical uncertainties of the branching ratios could be largely canceled in the ratio of the branching ratios of  $B_s \rightarrow \phi \ell^+ \ell^-$  decays, one can define and check the physical observables  $R_\phi^{e\mu}$  and  $R_\phi^{\mu\tau}$  [5]. In the region  $q^2 < 4m_\mu^2$ , where only the  $e^+e^-$  modes are allowed, there is a large enhancement due to the  $1/q^2$  scaling of the photon penguin contribution [89]. In order to remove the phase space effects in the ratio  $R_\phi^{e\mu}$  and keep consistent with other analysis [5], we here also use the lower cut of  $4m_\mu^2$  for both the electron and muon modes in the definition of the ratio  $R_\phi^{e\mu}$  as in Ref. [5]:

$$R_\phi^{e\mu} = \frac{\int_{4m_\mu^2}^{q_{max}^2} dq^2 \frac{d\mathcal{B}(B_s \rightarrow \phi \mu^+ \mu^-)}{dq^2}}{\int_{4m_\mu^2}^{q_{max}^2} dq^2 \frac{d\mathcal{B}(B_s \rightarrow \phi e^+ e^-)}{dq^2}} = \begin{cases} 0.992 \pm 0.002, & \text{in PQCD,} \\ 0.991 \pm 0.002, & \text{in PQCD + Lattice,} \end{cases} \quad (46)$$

For the case of the ratio  $R_\phi^{\mu\tau}$  we have

$$R_\phi^{\mu\tau} = \frac{\int_{4m_\tau^2}^{q_{max}^2} dq^2 \frac{d\mathcal{B}(B_s \rightarrow \phi \tau^+ \tau^-)}{dq^2}}{\int_{4m_\mu^2}^{q_{max}^2} dq^2 \frac{d\mathcal{B}(B_s \rightarrow \phi \mu^+ \mu^-)}{dq^2}} = \begin{cases} 0.115 \pm 0.004, & \text{in PQCD,} \\ 0.100 \pm 0.009, & \text{in PQCD + Lattice,} \end{cases} \quad (47)$$

where the total error is the combination of the individual errors in quadrature. We suggest the LHCb and Belle-II to measure these two ratios.

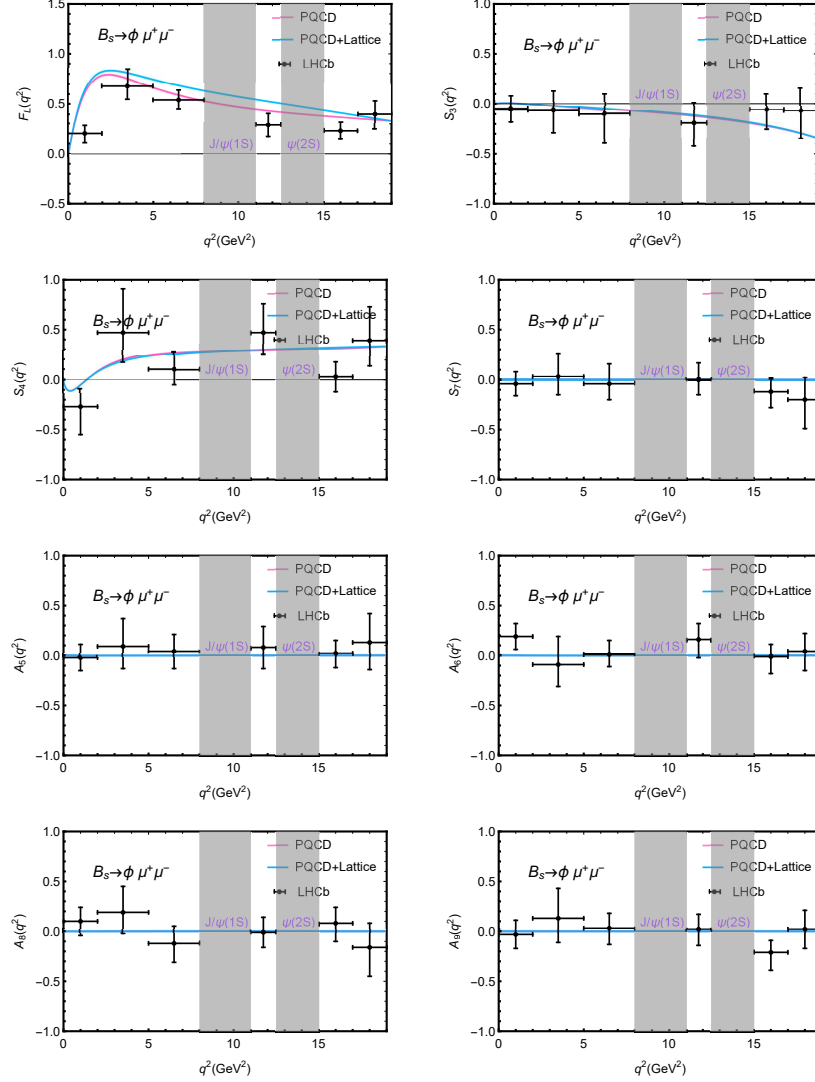


FIG. 3: Theoretical predictions for the  $q^2$ -dependence of the observables  $F_L(q^2)$ ,  $S_{3,4,7}(q^2)$  and  $A_{5,6,8,9}(q^2)$  for the decay  $B_s \rightarrow \phi \mu^+ \mu^-$  in the PQCD ( red lines ) and “PQCD+Lattice” ( blue lines ) approach. The crosses in each figure represent the LHCb measurements in six  $q^2$  bins [31]. The vertical grey blocks are the two experimental veto regions.

For  $B_s \rightarrow \phi \mu^+ \mu^-$  decay, we show the PQCD and “PQCD+Lattice” predictions for the  $q^2$ -dependence of the longitudinal polarization  $F_L(q^2)$ , the CP averaged angular coefficients  $S_{3,4,7}(q^2)$  and the CP asymmetry angular coefficients  $A_{5,6,8,9}(q^2)$  in Fig. 3. As a comparison, the currently available LHCb measurements for these observables of  $B_s \rightarrow \phi \mu^+ \mu^-$  decay in the six  $q^2$  bins [31] are also shown by those crosses explicitly. One can see from the Fig. 3 that:

- (1) For the longitudinal polarization  $F_L(q^2)$ , although both PQCD and “PQCD+Lattice” predictions all agree well with the LHCb measurements in the six bins, our theoretical predictions in the region of the fourth and fifth bin are little larger than the measured ones.
- (2) For the CP averaged angular coefficients  $S_{3,4,7}(q^2)$ , the PQCD and “PQCD+Lattice”

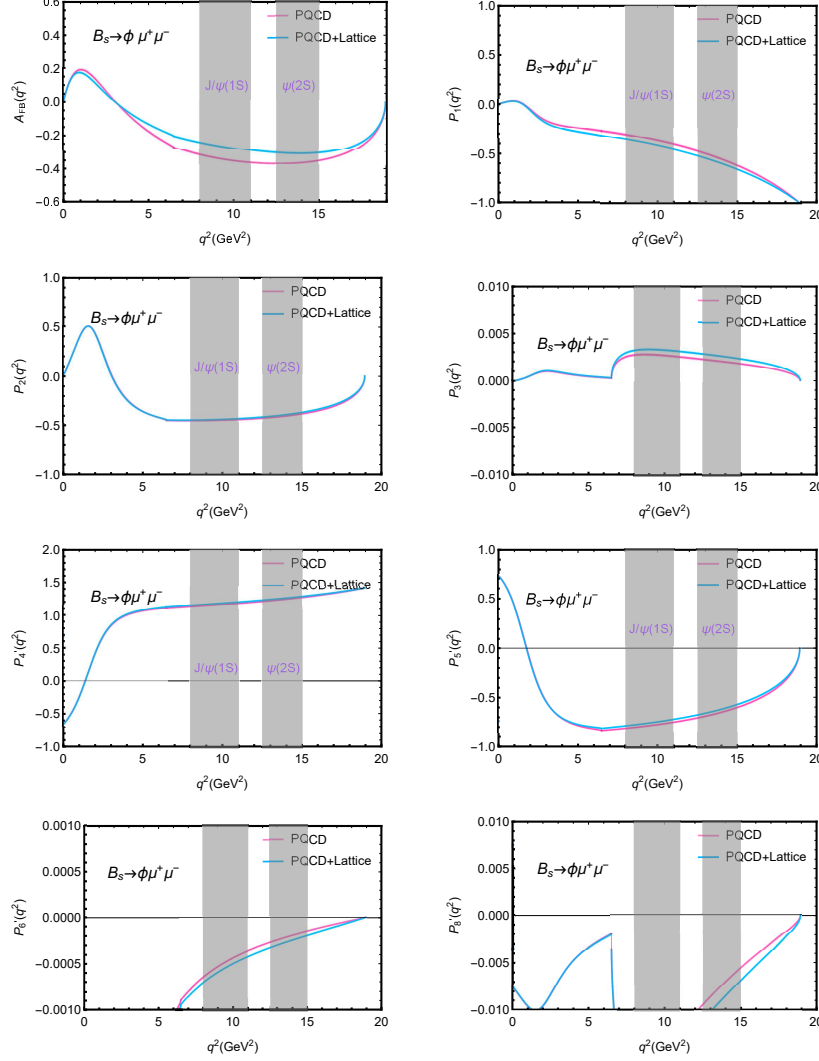


FIG. 4: Theoretical predictions for the  $q^2$ -dependence of the observables  $A_{FB}(q^2)$ ,  $P_{1,2,3}(q^2)$  and  $P'_{4,5,6,8}(q^2)$  for  $B_s \rightarrow \phi \mu^+ \mu^-$  decay in the PQCD (red lines) and “PQCD+Lattice” (blue lines) approach. The vertical grey blocks are the two experimental veto regions.

predictions agree very well with each other, and are consistent with the LHCb results within the still large experimental errors. For the last two high  $q^2$  bins, the LHCb results of  $S_3$  ( $S_7$ ) is a little larger (smaller) than our theoretical predictions.

- (3) For the CP asymmetry angular coefficients  $A_{5,6,8,9}(q^2)$ , the PQCD and “PQCD+Lattice” predictions are very small: in the range of  $\sim 10^{-4}$  to  $10^{-2}$ . For the LHCb measurements in the six bins, they are clearly consistent with our theoretical predictions due to still large experimental errors !

In Fig. 4, we show the PQCD and “PQCD+Lattice” predictions for the  $q^2$ -dependence of the forward-backward asymmetry  $A_{FB}(q^2)$ , the optimized observables  $P_{1,2,3}(q^2)$  and  $P'_{4,5,6,8}(q^2)$  for  $B_s \rightarrow \phi \mu^+ \mu^-$  decay. Unfortunately, there exist no any experimental measurements for these observables. We have to wait for future LHCb and Belle-II measurements. Analogous to Fig. 2, the vertical grey blocks in both Fig. 3 and 4 also denote the

two experimental veto regions of  $q^2$ :  $8.0 < q^2 < 11.0 \text{ GeV}^2$  and  $12.5 < q^2 < 15.0 \text{ GeV}^2$ .

TABLE VI: Theoretical predictions for the observables  $F_L^\phi$ ,  $A_{FB}$ ,  $S_{3,4,7}$ ,  $A_{5,6,8,9}$ ,  $P_{1,2,3}$  and  $P'_{4,5,6,8}$  integrated over the whole kinematic region for  $B_s \rightarrow \phi \ell^+ \ell^-$  decays in the PQCD (the first row) and “PQCD+Lattice” (the second row) approaches, respectively.

Obs.	$\ell = e$	$\ell = \mu$	$\ell = \tau$	Obs.	$\ell = e$	$\ell = \mu$	$\ell = \tau$
$F_L^\phi$	$0.383^{+0.003}_{-0.004}$	$0.454^{+0.006}_{-0.007}$	$0.396^{+0.002}_{-0.003}$	$-A_{FB}$	$0.192^{+0.003}_{-0.004}$	$0.233^{+0.004}_{-0.004}$	$0.173^{+0.002}_{-0.002}$
	$0.446^{+0.012}_{-0.013}$	$0.533^{+0.001}_{-0.001}$	$0.442^{+0.002}_{-0.002}$		$0.152^{+0.010}_{-0.008}$	$0.186^{+0.005}_{-0.004}$	$0.151^{+0.002}_{-0.003}$
$-S_3$	$0.120^{+0.005}_{-0.004}$	$0.144^{+0.005}_{-0.005}$	$0.080^{+0.001}_{-0.001}$	$-P_1$	$0.399^{+0.014}_{-0.011}$	$0.555^{+0.010}_{-0.012}$	$0.795^{+0.007}_{-0.004}$
	$0.102^{+0.009}_{-0.008}$	$0.124^{+0.007}_{-0.006}$	$0.075^{+0.001}_{-0.001}$		$0.381^{+0.041}_{-0.039}$	$0.564^{+0.026}_{-0.024}$	$0.817^{+0.007}_{-0.005}$
$S_4$	$0.210^{+0.004}_{-0.004}$	$0.258^{+0.003}_{-0.004}$	$0.100^{+0.001}_{-0.001}$	$-P_2$	$0.213^{+0.002}_{-0.003}$	$0.299^{+0.001}_{-0.001}$	$0.281^{+0.003}_{-0.004}$
	$0.201^{+0.012}_{-0.013}$	$0.249^{+0.007}_{-0.006}$	$0.098^{+0.001}_{-0.001}$		$0.189^{+0.015}_{-0.013}$	$0.282^{+0.005}_{-0.004}$	$0.268^{+0.004}_{-0.004}$
$10^3 S_7$	$0.350^{+0.010}_{-0.011}$	$0.371^{+0.012}_{-0.013}$	$0.022^{+0.001}_{-0.000}$	$10^2 P_3$	$0.103^{+0.003}_{-0.006}$	$0.142^{+0.002}_{-0.007}$	$0.122^{+0.003}_{-0.006}$
	$0.392^{+0.026}_{-0.024}$	$0.423^{+0.040}_{-0.035}$	$0.030^{+0.001}_{-0.000}$		$0.118^{+0.012}_{-0.012}$	$0.174^{+0.007}_{-0.008}$	$0.158^{+0.002}_{-0.003}$
$-10^3 A_5$	$0.489^{+0.010}_{-0.009}$	$0.585^{+0.012}_{-0.013}$	$0.040^{+0.000}_{-0.000}$	$P'_4$	$1.049^{+0.013}_{-0.015}$	$1.111^{+0.011}_{-0.012}$	$1.338^{+0.002}_{-0.002}$
	$0.518^{+0.020}_{-0.020}$	$0.623^{+0.041}_{-0.046}$	$0.038^{+0.001}_{-0.001}$		$1.033^{+0.033}_{-0.037}$	$1.098^{+0.024}_{-0.027}$	$1.345^{+0.002}_{-0.003}$
$-10^3 A_6$	$0.482^{+0.001}_{-0.001}$	$0.577^{+0.002}_{-0.004}$	$0.068^{+0.000}_{-0.001}$	$-P'_5$	$0.482^{+0.002}_{-0.004}$	$0.524^{+0.003}_{-0.005}$	$0.427^{+0.005}_{-0.006}$
	$0.429^{+0.020}_{-0.021}$	$0.518^{+0.038}_{-0.043}$	$0.058^{+0.001}_{-0.001}$		$0.470^{+0.008}_{-0.010}$	$0.515^{+0.002}_{-0.003}$	$0.408^{+0.006}_{-0.006}$
$10^4 A_8$	$0.541^{+0.030}_{-0.027}$	$0.241^{+0.017}_{-0.020}$	$0.011^{+0.000}_{-0.000}$	$-10^3 P'_6$	$0.875^{+0.031}_{-0.030}$	$0.780^{+0.028}_{-0.029}$	$0.069^{+0.001}_{-0.001}$
	$0.550^{+0.088}_{-0.095}$	$0.237^{+0.060}_{-0.070}$	$0.014^{+0.000}_{-0.000}$		$1.007^{+0.089}_{-0.101}$	$0.910^{+0.078}_{-0.089}$	$0.097^{+0.001}_{-0.001}$
$10^4 A_9$	$0.040^{+0.002}_{-0.004}$	$0.054^{+0.002}_{-0.004}$	$0.013^{+0.001}_{-0.001}$	$-10^2 P'_8$	$0.643^{+0.009}_{-0.003}$	$0.640^{+0.004}_{-0.008}$	$0.287^{+0.002}_{-0.002}$
	$0.041^{+0.006}_{-0.008}$	$0.056^{+0.004}_{-0.007}$	$0.015^{+0.001}_{-0.001}$		$0.749^{+0.004}_{-0.004}$	$0.748^{+0.006}_{-0.006}$	$0.374^{+0.001}_{-0.001}$

In Table VI, we list the theoretical predictions for the values of the observables  $F_L^\phi$ ,  $A_{FB}$ ,  $S_{3,4,7}$ ,  $A_{5,6,8,9}$ ,  $P_{1,2,3}$  and  $P'_{4,5,6,8}$ , obtained after the integrations over the whole kinematic region of  $q^2$  for the semileptonic decays  $B_s \rightarrow \phi \ell^+ \ell^-$  with  $\ell = (e, \mu, \tau)$  in the PQCD (the first row) and “PQCD+Lattice” (the second row) approaches, respectively. Of course, the regions corresponding to resonance  $J/\psi(1S)$  and  $\psi(2S)$ , say  $8.0 < q^2 < 11.0 \text{ GeV}^2$  and  $12.5 < q^2 < 15.0 \text{ GeV}^2$  numerically, are also cut off here. The total errors are the combinations of the individual errors from the form factors, the renormalization scales and the relevant CKM matrix elements. The above theoretical predictions should be tested in the near future LHCb and Belle-II experiments. For the considered  $B_s$  meson decays, one should consider the effects from the  $B_s$ - $\bar{B}_s$  mixing [6]. The theoretical framework for examining the time-dependent decays with the inclusion of such mixing effects can be found in Ref. [90]. The authors of Ref. [90] proved that the mixing effects on the values of decay rates and CP averaged observables are generally within a few percent and could be neglected.

### C. The $q^2$ -binned observables

For  $B_s \rightarrow \phi \mu^+ \mu^-$  decay mode, the LHCb Collaboration has reported their experimental measurements for many physical observables in several  $q^2$  bins [31]. In order to compare our theoretical predictions with the LHCb results bin by bin, we make the same choices of the  $q^2$  bins as LHCb did, calculate and show our theoretical predictions for the branching ratio  $\mathcal{B}(B_s \rightarrow \phi \ell^+ \ell^-)$  and the asymmetry  $F_L^\phi$  with  $\ell = (\mu, \tau)$  in Table VII, and the observables

TABLE VII: Theoretical predictions for the  $q^2$ -binned observables  $\mathcal{B}(B_s \rightarrow \phi \ell^+ \ell^-)$  (in unit of  $10^{-7}$ ) and  $F_L^\phi$  with  $\ell = (\mu, \tau)$  in the PQCD (the first low) and “PQCD+Lattice” (the second row) approach, respectively. For a comparison, we also list the experiment measurements for the  $q^2$ -binned results from the LHCb Collaboration [31].

$q^2$ bin (GeV <sup>2</sup> )	$\mathcal{B}(\ell = \mu)$	LHCb	$\mathcal{B}(\ell = \tau)$	$F_L^\phi(\ell = \mu)$	LHCb	$F_L^\phi(\ell = \tau)$
[0.1, 2.0]	$0.39^{+0.16}_{-0.11}$	$1.11 \pm 0.16$	—	$0.441^{+0.007}_{-0.008}$	$0.20 \pm 0.09$	—
	$0.40^{+0.16}_{-0.11}$			$0.472^{+0.011}_{-0.012}$		
[2.0, 5.0]	$0.48^{+0.20}_{-0.14}$	$0.77 \pm 0.14$	—	$0.738^{+0.008}_{-0.009}$	$0.68 \pm 0.15$	—
	$0.58^{+0.18}_{-0.13}$			$0.796^{+0.007}_{-0.007}$		
[5.0, 8.0]	$0.84^{+0.37}_{-0.25}$	$0.96 \pm 0.15$	—	$0.584^{+0.008}_{-0.009}$	$0.54 \pm 0.10$	—
	$0.96^{+0.25}_{-0.19}$			$0.682^{+0.010}_{-0.008}$		
[11.0, 12.5]	$0.78^{+0.38}_{-0.25}$	$0.71 \pm 0.12$	—	$0.433^{+0.003}_{-0.005}$	$0.29 \pm 0.11$	—
	$0.76^{+0.14}_{-0.11}$			$0.524^{+0.008}_{-0.008}$		
[15.0, 17.0]	$1.12^{+0.61}_{-0.40}$	$0.90 \pm 0.13$	$0.45^{+0.22}_{-0.14}$	$0.368^{+0.001}_{-0.001}$	$0.23 \pm 0.09$	$0.421^{+0.003}_{-0.004}$
	$0.99^{+0.11}_{-0.10}$		$0.39^{+0.04}_{-0.04}$	$0.412^{+0.004}_{-0.004}$		$0.479^{+0.003}_{-0.003}$
[17.0, 19.0]	$0.80^{+0.41}_{-0.27}$	$0.75 \pm 0.13$	$0.36^{+0.18}_{-0.12}$	$0.346^{+0.001}_{-0.001}$	$0.40 \pm 0.14$	$0.365^{+0.001}_{-0.002}$
	$0.67^{+0.05}_{-0.05}$		$0.29^{+0.02}_{-0.02}$	$0.363^{+0.001}_{-0.001}$		$0.391^{+0.001}_{-0.001}$
[1.0, 6.0]	$0.93^{+0.29}_{-0.27}$	$1.29 \pm 0.19$	—	$0.708^{+0.007}_{-0.009}$	$0.63 \pm 0.09$	—
	$1.10^{+0.34}_{-0.25}$			$0.777^{+0.008}_{-0.006}$		
[15.0, 19.0]	$1.99^{+1.02}_{-0.71}$	$1.62 \pm 0.20$	$0.82^{+0.40}_{-0.26}$	$0.359^{+0.002}_{-0.001}$	$0.29 \pm 0.07$	$0.396^{+0.003}_{-0.003}$
	$1.60^{+0.16}_{-0.16}$		$0.68^{+0.06}_{-0.06}$	$0.394^{+0.003}_{-0.003}$		$0.442^{+0.002}_{-0.001}$

$S_{3,4,7}$  with  $\ell = \mu$  in Table VIII. For observables  $S_7$ ,  $A_{5,6,8,9}$ , in fact, our theoretical predictions for their values are very small, say in the range of  $10^{-3} - 10^{-4}$  in magnitude, but still agree with the LHCb measurements in different bins [31] due to still large experimental errors. For the observables  $P_3$  and  $P'_{6,8}$ , they are also very small in size: in the range of  $10^{-3} - 10^{-4}$  and there exist no corresponding data at present. Since the magnitude of the observables  $A_{5,6,8,9}$ ,  $P_3$  and  $P'_{6,8}$  are too small to be measured in recent years, we do not make further comparative studies on them bin by bin. For observables  $A_{FB}$ ,  $P_{1,2}$  and  $P'_{4,5}$ , on the other hand, although there exist no experimental measurements for them at present, they are relatively large in size and may be measured in the near future LHCb and Belle-II experiments, so we calculate and list the theoretical predictions of these observables bin by bin for the cases of  $\ell = (\mu, \tau)$  in Table IX and X.

The definitions of the  $q^2$ -binned observables are the following:

$$\mathcal{B}(q_1^2, q_2^2) = \int_{q_1^2}^{q_2^2} dq^2 \frac{d\mathcal{B}(B_s \rightarrow \phi \ell^+ \ell^-)}{dq^2}, \quad F_L^\phi(q_1^2, q_2^2) = \frac{\int_{q_1^2}^{q_2^2} dq^2 [3(I_1^c + \bar{I}_1^c) - (I_2^c + \bar{I}_2^c)]}{4 \int_{q_1^2}^{q_2^2} dq^2 [d(\Gamma + \bar{\Gamma})/dq^2]}, \quad (48)$$

$$A_{FB}(q_1^2, q_2^2) = \frac{3 \int_{q_1^2}^{q_2^2} dq^2 (I_6^s + \bar{I}_6^s)}{4 \int_{q_1^2}^{q_2^2} dq^2 [d(\Gamma + \bar{\Gamma})/dq^2]}, \quad S_{3,4,7}(q_1^2, q_2^2) = \frac{\int_{q_1^2}^{q_2^2} dq^2 (I_{3,4,7} + \bar{I}_{3,4,7})}{\int_{q_1^2}^{q_2^2} dq^2 [d(\Gamma + \bar{\Gamma})/dq^2]}, \quad (49)$$

TABLE VIII: Theoretical predictions for the  $q^2$ -binned observables  $S_{3,4,7}$  of the decays  $B_s \rightarrow \phi\mu^+\mu^-$  in the PQCD (the first low) and “PQCD+Lattice” (the second row) approaches. For a comparison, we also list the LHCb measured values [31].

$q^2$ bin (GeV <sup>2</sup> )	$S_3$		$S_4$		$S_7$	
	Theor.	LHCb	Theor.	LHCb	Theor. ( $10^{-3}$ )	LHCb
[0.1, 2.0]	$0.003^{+0.000}_{-0.000}$ $0.002^{+0.000}_{-0.001}$	$-0.05 \pm 0.13$	$-0.054^{+0.001}_{-0.001}$ $-0.053^{+0.000}_{-0.000}$	$-0.27 \pm 0.23$	$1.571^{+0.001}_{-0.002}$ $1.551^{+0.003}_{-0.006}$	$-0.04 \pm 0.12$
[2.0, 5.0]	$-0.024^{+0.002}_{-0.002}$ $-0.021^{+0.001}_{-0.001}$	$-0.06 \pm 0.21$	$0.191^{+0.004}_{-0.004}$ $0.177^{+0.003}_{-0.003}$	$0.47 \pm 0.37$	$1.065^{+0.003}_{-0.003}$ $0.979^{+0.017}_{-0.018}$	$0.03 \pm 0.21$
[5.0, 8.0]	$-0.057^{+0.003}_{-0.003}$ $-0.050^{+0.004}_{-0.003}$	$-0.10 \pm 0.25$	$0.270^{+0.002}_{-0.002}$ $0.259^{+0.003}_{-0.003}$	$0.10 \pm 0.17$	$0.453^{+0.003}_{-0.003}$ $0.453^{+0.004}_{-0.005}$	$-0.04 \pm 0.18$
[11.0, 12.5]	$-0.124^{+0.004}_{-0.003}$ $-0.115^{+0.002}_{-0.001}$	$-0.19 \pm 0.21$	$0.296^{+0.001}_{-0.001}$ $0.303^{+0.001}_{-0.001}$	$0.47 \pm 0.25$	$0.153^{+0.002}_{-0.002}$ $0.185^{+0.001}_{-0.001}$	$0.00 \pm 0.16$
[15.0, 17.0]	$-0.219^{+0.003}_{-0.003}$ $-0.213^{+0.001}_{-0.001}$	$-0.06 \pm 0.18$	$0.314^{+0.001}_{-0.001}$ $0.323^{+0.001}_{-0.001}$	$0.03 \pm 0.15$	$0.052^{+0.001}_{-0.001}$ $0.071^{+0.001}_{-0.001}$	$-0.12 \pm 0.15$
[17.0, 19.0]	$-0.283^{+0.001}_{-0.001}$ $-0.281^{+0.001}_{-0.001}$	$-0.07 \pm 0.25$	$0.325^{+0.001}_{-0.001}$ $0.329^{+0.001}_{-0.001}$	$0.39 \pm 0.30$	$0.019^{+0.001}_{-0.001}$ $0.027^{+0.001}_{-0.001}$	$-0.20 \pm 0.26$
[1.0, 6.0]	$-0.026^{+0.002}_{-0.002}$ $-0.023^{+0.001}_{-0.001}$	$-0.02 \pm 0.13$	$0.180^{+0.004}_{-0.004}$ $0.169^{+0.001}_{-0.001}$	$0.19 \pm 0.14$	$1.063^{+0.001}_{-0.001}$ $0.985^{+0.020}_{-0.022}$	$0.03 \pm 0.14$
[15.0, 19.0]	$-0.245^{+0.002}_{-0.002}$ $-0.239^{+0.001}_{-0.001}$	$-0.09 \pm 0.12$	$0.318^{+0.001}_{-0.001}$ $0.325^{+0.001}_{-0.001}$	$0.14 \pm 0.11$	$0.038^{+0.002}_{-0.002}$ $0.054^{+0.001}_{-0.001}$	$-0.13 \pm 0.11$

$$P_1(q_1^2, q_2^2) = \frac{\int_{q_1^2}^{q_2^2} dq^2 (S_3)}{2 \int_{q_1^2}^{q_2^2} dq^2 (S_2^s)}, \quad P_2(q_1^2, q_2^2) = \frac{\int_{q_1^2}^{q_2^2} dq^2 (\beta_\ell S_6^s)}{8 \int_{q_1^2}^{q_2^2} dq^2 (S_2^s)}, \quad (50)$$

$$P'_4(q_1^2, q_2^2) = \frac{\int_{q_1^2}^{q_2^2} dq^2 (S_4)}{\sqrt{-\int_{q_1^2}^{q_2^2} dq^2 (S_2^c S_2^s)}}, \quad P'_5(q_1^2, q_2^2) = \frac{\int_{q_1^2}^{q_2^2} dq^2 (\beta_\ell S_5^s)}{2 \sqrt{-\int_{q_1^2}^{q_2^2} dq^2 (S_2^c S_2^s)}}. \quad (51)$$

From the numerical values as shown in Fig. 3 and in Table VII and VIII, we find the following points about the relevant physical observables of the considered  $B_s \rightarrow \phi\mu^+\mu^-$  decays in bins:

- (1) For  $B_s \rightarrow \phi\mu^+\mu^-$  decay, besides the good consistency between the theory and the LHCb data for the integrated total branching ratio  $\mathcal{B}(B_s \rightarrow \phi\mu^+\mu^-)$  as listed in Eq. (45), the PQCD and “PQCD+Lattice” predictions for  $\mathcal{B}(B_s \rightarrow \phi\mu^+\mu^-)$  in most bins do agree well with the measured ones within  $2\sigma$  errors. For the first low- $q^2$  bin  $0.1 < q^2 < 2$  (GeV<sup>2</sup>), however, the central value of the LHCb result  $1.11 \pm 0.16$  is larger than the theoretical ones by roughly a factor of three. The LHCb results of  $\mathcal{B}(B_s \rightarrow \phi\mu^+\mu^-)$  in different bins of  $q^2$  as listed in the third column of Table VII are obtained from the results in Table I of Ref. [31] by multiplying the LHCb measured values of differential decay rate  $d\mathcal{B}(B_s \rightarrow \phi\mu^+\mu^-)/dq^2$  with the width of the corresponding bin ( $q_2^2 - q_1^2$ ). The theoretical errors of our theoretical predictions

TABLE IX: Theoretical predictions for the  $q^2$ -binned observables  $A_{FB}^\mu$ ,  $P_{1,2}$  of the decays  $B_s \rightarrow \phi \ell^+ \ell^-$  with  $\ell = (\mu, \tau)$  in the PQCD (the first low) and “PQCD+Lattice” (the second row) approaches.

$q^2$ bin (GeV <sup>2</sup> )	$A_{FB}^\mu$	$A_{FB}^\tau$	$P_1(\ell = \mu)$	$P_1(\ell = \tau)$	$P_2(\ell = \mu)$	$P_2(\ell = \tau)$
[0.1, 2.0]	$0.131^{+0.003}_{-0.003}$	—	$0.015^{+0.001}_{-0.001}$	—	$0.206^{+0.001}_{-0.001}$	—
	$0.122^{+0.003}_{-0.002}$	—	$0.013^{+0.001}_{-0.001}$	—	$0.204^{+0.001}_{-0.001}$	—
[2.0, 5.0]	$-0.047^{+0.004}_{-0.003}$	—	$-0.197^{+0.007}_{-0.007}$	—	$-0.128^{+0.003}_{-0.003}$	—
	$-0.038^{+0.001}_{-0.002}$	—	$-0.225^{+0.005}_{-0.006}$	—	$-0.132^{+0.002}_{-0.002}$	—
[5.0, 8.0]	$-0.265^{+0.006}_{-0.005}$	—	$-0.280^{+0.009}_{-0.008}$	—	$-0.431^{+0.001}_{-0.001}$	—
	$-0.200^{+0.006}_{-0.006}$	—	$-0.323^{+0.003}_{-0.004}$	—	$-0.427^{+0.001}_{-0.001}$	—
[11.0, 12.5]	$-0.365^{+0.001}_{-0.001}$	—	$-0.440^{+0.010}_{-0.008}$	—	$-0.431^{+0.002}_{-0.003}$	—
	$-0.298^{+0.005}_{-0.005}$	—	$-0.489^{+0.002}_{-0.003}$	—	$-0.420^{+0.001}_{-0.001}$	—
[15.0, 17.0]	$-0.326^{+0.001}_{-0.001}$	$-0.188^{+0.001}_{-0.001}$	$-0.697^{+0.009}_{-0.006}$	$-0.707^{+0.009}_{-0.005}$	$-0.345^{+0.003}_{-0.004}$	$-0.341^{+0.003}_{-0.004}$
	$-0.290^{+0.005}_{-0.005}$	$-0.160^{+0.003}_{-0.003}$	$-0.730^{+0.007}_{-0.005}$	$-0.738^{+0.006}_{-0.006}$	$-0.330^{+0.003}_{-0.003}$	$-0.326^{+0.003}_{-0.004}$
[17.0, 19.0]	$-0.226^{+0.002}_{-0.003}$	$-0.153^{+0.001}_{-0.002}$	$-0.869^{+0.005}_{-0.003}$	$-0.875^{+0.005}_{-0.003}$	$-0.231^{+0.002}_{-0.003}$	$-0.225^{+0.003}_{-0.004}$
	$-0.208^{+0.004}_{-0.003}$	$-0.137^{+0.003}_{-0.002}$	$-0.884^{+0.004}_{-0.004}$	$-0.890^{+0.005}_{-0.003}$	$-0.219^{+0.003}_{-0.004}$	$-0.213^{+0.004}_{-0.004}$

TABLE X: Theoretical predictions for the  $q^2$ -binned optimized observables  $P'_4$  and  $P'_5$  of the decays  $B_s \rightarrow \phi \ell^+ \ell^-$  with  $\ell = (e, \mu, \tau)$  in the PQCD (the first low) and “PQCD+Lattice” (the second row) approach.

$q^2$ bin (GeV <sup>2</sup> )	$P'_4(\ell = e)$	$P'_4(\ell = \mu)$	$P'_4(\ell = \tau)$	$P'_5(\ell = e)$	$P'_5(\ell = \mu)$	$P'_5(\ell = \tau)$
[0.1, 2.0]	$-0.322^{+0.005}_{-0.005}$	$-0.289^{+0.005}_{-0.005}$	—	$0.484^{+0.001}_{-0.002}$	$0.459^{+0.001}_{-0.002}$	—
	$-0.318^{+0.001}_{-0.001}$	$-0.285^{+0.001}_{-0.001}$	—	$0.475^{+0.002}_{-0.001}$	$0.449^{+0.001}_{-0.001}$	—
[2.0, 5.0]	$0.903^{+0.007}_{-0.007}$	$0.903^{+0.007}_{-0.007}$	—	$-0.606^{+0.001}_{-0.002}$	$-0.607^{+0.001}_{-0.002}$	—
	$0.916^{+0.001}_{-0.001}$	$0.916^{+0.001}_{-0.001}$	—	$-0.608^{+0.004}_{-0.003}$	$-0.608^{+0.004}_{-0.004}$	—
[5.0, 8.0]	$1.110^{+0.003}_{-0.005}$	$1.110^{+0.004}_{-0.005}$	—	$-0.816^{+0.005}_{-0.006}$	$-0.816^{+0.005}_{-0.006}$	—
	$1.127^{+0.002}_{-0.001}$	$1.127^{+0.002}_{-0.001}$	—	$-0.796^{+0.003}_{-0.001}$	$-0.796^{+0.002}_{-0.002}$	—
[11.0, 12.5]	$1.198^{+0.002}_{-0.005}$	$1.198^{+0.002}_{-0.005}$	—	$-0.727^{+0.005}_{-0.007}$	$-0.727^{+0.005}_{-0.007}$	—
	$1.217^{+0.001}_{-0.001}$	$1.217^{+0.001}_{-0.001}$	—	$-0.698^{+0.001}_{-0.001}$	$-0.698^{+0.002}_{-0.001}$	—
[15.0, 17.0]	$1.302^{+0.002}_{-0.004}$	$1.302^{+0.002}_{-0.004}$	$1.306^{+0.002}_{-0.004}$	$-0.533^{+0.005}_{-0.007}$	$-0.533^{+0.005}_{-0.007}$	$-0.525^{+0.006}_{-0.008}$
	$1.314^{+0.002}_{-0.003}$	$1.314^{+0.002}_{-0.003}$	$1.317^{+0.003}_{-0.002}$	$-0.506^{+0.005}_{-0.006}$	$-0.506^{+0.005}_{-0.006}$	$-0.498^{+0.006}_{-0.006}$
[17.0, 19.0]	$1.366^{+0.001}_{-0.002}$	$1.366^{+0.001}_{-0.002}$	$1.369^{+0.001}_{-0.002}$	$-0.341^{+0.004}_{-0.006}$	$-0.341^{+0.004}_{-0.006}$	$-0.331^{+0.004}_{-0.006}$
	$1.371^{+0.001}_{-0.001}$	$1.371^{+0.001}_{-0.001}$	$1.374^{+0.001}_{-0.002}$	$-0.323^{+0.005}_{-0.006}$	$-0.323^{+0.005}_{-0.006}$	$-0.314^{+0.006}_{-0.006}$

of the branching ratios in bins are still relatively large, while the differences between the PQCD and “PQCD+Lattice” predictions for  $\mathcal{B}(B_s \rightarrow \phi \ell^+ \ell^-)$  with  $\ell = (\mu, \tau)$  are small.

- (2) In the first low- $q^2$  bin  $0.1 < q^2 < 2$  (GeV<sup>2</sup>), both the PQCD and “PQCD+Lattice” predictions for  $F_L^\phi(\ell = \mu)$  are larger than the LHCb measured results  $F_L^\phi(\ell = \mu)|_{\text{LHCb}} = 0.20^{+0.08}_{-0.09} \pm 0.02$  [31]. For other bins, both the PQCD and “PQCD+Lattice” predictions of  $F_L^\phi$  for muon mode do agree very well with currently available LHCb measured values

[31] within  $2\sigma$  errors. It is worth of remaining that our theoretical predictions of  $F_L^\phi$  have a little error of  $\sim 2\%$  due to the strong cancellation of the theoretical errors in the ratios. The theoretical predictions for  $\mathcal{B}(B_s \rightarrow \phi\tau^+\tau^-)$  and  $F_L^\phi(\ell = \tau)$  in different bins of  $q^2$  as listed in Table VII will be tested by future experimental measurements,

- (3) For the observables  $S_{3,4,7}$ , as listed in Table VIII, the PQCD and “PQCD+Lattice” predictions for their values in all bins are in the range of  $10^{-3} - 10^{-1}$ , and show a good agreement with the LHCb measured values [31]. The theoretical errors of the PQCD and “PQCD+Lattice” predictions are also very small,  $\sim 2\%$  in magnitude, because of their nature as the ratios. In all bins, the LHCb measured values of  $S_{3,4,7}$  are still consistent with zero due to their still large errors, which is a clear feature as can be seen easily from the numerical values in Table VIII and the crosses in Fig. 3.

In Table IX and X, we show the PQCD and “PQCD+Lattice” predictions for the physical observables  $A_{FB}^{\mu,\tau}$ ,  $P_{1,2}^{\mu,\tau}$  and  $P'_{4,5}(\ell = e, \mu, \tau)$  in six bins. Although there exist no experimental measurements for these physical observables at present, we do believe that these predictions could be tested in the near future LHCb and Belle-II experiments.

## V. SUMMARY

In this paper, we made a systematic study of the semileptonic decays  $B_s \rightarrow \phi\ell^+\ell^-$  with  $\ell^- = (e^-, \mu^-, \tau^-)$  using the PQCD and the “PQCD+Lattice” factorization approach respectively. We first evaluated all relevant form factors in the low  $q^2$  region using the PQCD approach, and we also took currently available lattice QCD results at the high- $q^2$  points  $q^2 = (12, 16, 18.9) \text{ GeV}^2$  as additional input to improve the extrapolation of the form factors from the low to the high- $q^2$  region. We calculated the branching ratios  $\mathcal{B}(B_s \rightarrow \phi\ell^+\ell^-)$ , the CP averaged  $\phi$  longitudinal polarization fraction  $F_L(q^2)$ , the forward-backward asymmetry  $\mathcal{A}_{FB}(q^2)$ , the CP averaged angular coefficients  $S_{3,4,7}(q^2)$ , the CP asymmetry angular coefficients  $A_{5,6,8,9}(q^2)$ , the optimized observables  $P_{1,2,3}(q^2)$  and  $P'_{4,5,6,8}(q^2)$ . For  $B_s \rightarrow \phi\mu^+\mu^-$  decay mode, we calculated the binned values of the branching ratio  $\mathcal{B}(B_s \rightarrow \phi\mu^+\mu^-)$ , the observables  $F_L^\phi$  and  $S_{3,4,7}$  in the same bins as defined by LHCb Collaboration [31] in order to compare our theoretical predictions with those currently available LHCb measurements bin by bin directly.

Based on the analytical evaluations, the numerical results and the phenomenological analysis, we found the following main points:

- (1) For  $B_s \rightarrow \phi\mu^+\mu^-$  decay, both PQCD and “PQCD+Lattice” predictions of  $\mathcal{B}(B_s \rightarrow \phi\mu^+\mu^-)$  are about  $7 \times 10^{-7}$ , which agree well with the LHCb measured value  $(7.97^{+0.81}_{-0.80}) \times 10^{-7}$  and the QCDSR prediction  $(7.06 \pm 1.59) \times 10^{-7}$  within one standard deviation. For the electron and tau mode, our theoretical predictions for their decay rates are also well consistent with the corresponding QCDSR predictions and to be tested by future experimental measurements.
- (2) For the ratios of the branching ratios  $R_\phi^{e\mu}$  and  $R_\phi^{\mu\tau}$ , the PQCD and “PQCD+Lattice” predictions agree with each other and with small theoretical errors because of the strong cancellation of the theoretical errors in such ratios. We suggest the LHCb and Belle-II collaboration to measure these ratios.

- (3) For the longitudinal polarization  $F_L$ , both PQCD and "PQCD+Lattice" predictions agree with the LHCb measurements in the considered bins within the errors. For the CP averaged angular coefficients  $S_{3,4,7}$ , the PQCD and "PQCD+Lattice" predictions in all bins are small in magnitude, in the range of  $10^{-3} - 10^{-1}$ , and agree well with the LHCb results within the still large experimental errors. For the CP asymmetry angular coefficients  $A_{5,6,8,9}$ , the PQCD and "PQCD+Lattice" predictions are very small, in the range of  $10^{-4} - 10^{-2}$ , and clearly consistent with the LHCb measurements in the six bins.
- (4) For the physical observables  $A_{FB}^\ell$ ,  $P_{1,2,3}$  and  $P'_{4,5,6,8}$ , the experimental measurements are still absent now, we think that the PQCD and "PQCD+Lattice" predictions for these physical observables will be tested in the near future LHCb and Belle-II experiments.

### Acknowledgments

This work was supported by the National Natural Science Foundation of China under Grant No. 11775117 and 11235005.

### Appendix A: The transition form factors

In the framework of the PQCD factorization approach, the form factors  $V(q^2)$ ,  $A_{0,1,2}(q^2)$  and  $T_{1,2,3}$  of  $B_s \rightarrow \phi$  transition can be written in the following form:

$$\begin{aligned}
 V(q^2) = & 8\pi m_{B_s}^2 C_F (1+r) \int dx_1 dx_2 \int b_1 db_1 b_2 db_2 \phi_{B_s}(x_1) \\
 & \times \left\{ \left[ -x_2 r \phi_\phi^v(x_2) + \phi_\phi^T(x_2) + \frac{1+x_2 r \eta}{\sqrt{\eta^2-1}} \phi_\phi^a(x_2) \right] \cdot H_1(t_1) \right. \\
 & \left. + \left[ \left( r + \frac{x_1}{2\sqrt{\eta^2-1}} \right) \phi_\phi^v(x_2) - \frac{x_1 - 2r\eta}{2\sqrt{\eta^2-1}} \phi_\phi^a(x_2) \right] \cdot H_2(t_2) \right\}, \quad (A1)
 \end{aligned}$$

$$\begin{aligned}
 A_0(q^2) = & 8\pi m_{B_s}^2 C_F \int dx_1 dx_2 \int b_1 db_1 b_2 db_2 \phi_{B_s}(x_1) \times \left\{ \left[ (1+x_2 r (2\eta-r)) \phi_\phi(x_2) \right. \right. \\
 & \left. \left. + (1-2x_2) r \phi_\phi^t(x_2) + \frac{(1-r\eta) - 2x_2 r (\eta-r)}{\sqrt{\eta^2-1}} \phi_\phi^s(x_2) \right] \cdot H_1(t_1) \right. \\
 & \left. + \left[ \left[ \frac{x_1}{\sqrt{\eta^2-1}} \left( \frac{\eta+r}{2} - r\eta^2 \right) + \left( \frac{x_1}{2} - x_1 r \eta + r^2 \right) \right] \phi_\phi(x_2) \right. \right. \\
 & \left. \left. - \left[ \frac{x_1(1-r\eta) + 2r(r-\eta)}{\sqrt{\eta^2-1}} - x_1 r \right] \phi_\phi^s(x_2) \right] \cdot H_2(t_2) \right\}, \quad (A2)
 \end{aligned}$$

$$\begin{aligned}
 A_1(q^2) = & 16\pi m_{B_s}^2 C_F \frac{r}{1+r} \int dx_1 dx_2 \int b_1 db_1 b_2 db_2 \phi_{B_s}(x_1) \\
 & \times \left\{ \left[ (1+x_2 r \eta) \phi_\phi^v(x_2) + (\eta - 2x_2 r) \phi_\phi^T(x_2) + x_2 r \sqrt{\eta^2-1} \phi_\phi^a(x_2) \right] \cdot H_1(t_1) \right. \\
 & \left. + \left[ \left( r\eta - \frac{x_1}{2} \right) \phi_\phi^v(x_2) + \left( r\sqrt{\eta^2-1} + \frac{x_1}{2} \right) \phi_\phi^a(x_2) \right] \cdot H_2(t_2) \right\}, \quad (A3)
 \end{aligned}$$

$$\begin{aligned}
A_2(q^2) = & \frac{(1+r)^2(\eta-r)}{2r(\eta^2-1)} A_1(q^2) - 8\pi m_{B_s}^2 C_F \frac{1+r}{\eta^2-r} \int dx_1 dx_2 \int b_1 db_1 b_2 db_2 \phi_{B_s}(x_1) \\
& \times \left\{ \left[ \eta(1-x_2 r^2) + r(x_2(2\eta^2-1)-1) \right] \phi_\phi(x_2) + \left[ 1+2x_2 r^2 - (1+2x_2)r\eta \right] \phi_\phi^t(x_2) \right. \\
& + r(1-2x_2)\sqrt{\eta^2-1} \phi_\phi^s(x_2) \left. \right] \cdot H_1(t_1) \\
& + \left[ \left( r\eta - \frac{1}{2} \right) x_1 \sqrt{\eta^2-1} - \left[ r(r\eta-1-x_1\eta^2) + \frac{x_1(r+\eta)}{2} \right] \right] \phi_\phi(x_2) \\
& + \left[ x_1(r\eta-1) + (x_2-2)r\sqrt{\eta^2-1} \right] \phi_\phi^s(x_2) \left. \right] \cdot H_2(t_2) \Big\}, \tag{A4}
\end{aligned}$$

$$\begin{aligned}
T_1(q^2) = & 8\pi m_{B_s}^2 C_F \int dx_1 dx_2 \int b_1 db_1 b_2 db_2 \phi_{B_s}(x_1) \times \left\{ \left[ (1-2x_2)r\phi_\phi^v(x_2) \right. \right. \\
& + (1+2x_2 r\eta - x_2 r^2) \phi_\phi^T(x_2) + \frac{1+2x_2 r^2 - (1+2x_2)r\eta}{\sqrt{\eta^2-1}} \phi_\phi^a(x_2) \left. \right] \cdot H_1(t_1) \\
& + \left[ \left[ \left( 1 - \frac{x_1}{2} \right) r - \frac{x_1(r\eta-1)}{2\sqrt{\eta^2-1}} \right] \phi_\phi^v(x_2) + \left[ \frac{r(\eta-r)}{\sqrt{\eta^2-1}} + \frac{x_1}{2} \left( r + \frac{r\eta-1}{\sqrt{\eta^2-1}} \right) \right] \phi_\phi^a(x_2) \right] \cdot H_2(t_2) \Big\} \tag{A5}
\end{aligned}$$

$$\begin{aligned}
T_2(q^2) = & 16\pi m_{B_s}^2 C_F \frac{r}{1-r^2} \int dx_1 dx_2 \int b_1 db_1 b_2 db_2 \phi_{B_s}(x_1) \times \left\{ \left[ (1-(1+2x_2)r\eta+2x_2 r^2) \phi_\phi^v(x_2) \right. \right. \\
& + \left[ x_2 r\eta(2\eta-r) - x_2 r + \eta - r \right] \phi_\phi^T(x_2) + (1-2x_2)r\sqrt{\eta^2-1} \phi_\phi^a(x_2) \left. \right] \cdot H_1(t_1) \\
& + \left[ \left[ \frac{x_2}{2} \left( 1 + \frac{\eta}{\sqrt{\eta^2-1}} \right) (r\eta-1) + \left( r + \frac{x_1}{2\sqrt{\eta^2-1}} \right) (\eta-r) \right] \phi_\phi^v(x_2) \right. \\
& + \left. \left[ \left( 1 - \frac{x_1}{2} \right) r\sqrt{\eta^2-1} + \frac{x_1}{2} (1-r\eta) \right] \phi_\phi^a(x_2) \right] \cdot H_2(t_2) \Big\}, \tag{A6}
\end{aligned}$$

$$\begin{aligned}
T_3(q^2) = & \frac{(1-r)^2(\eta+r)}{2r(\eta^2-1)} T_2(q^2) - 8\pi m_{B_s}^2 C_F \frac{1-r^2}{\eta^2-1} \int dx_1 dx_2 \int b_1 db_1 b_2 db_2 \phi_{B_s}(x_1) \\
& \times \left\{ \left[ \frac{\eta^2 - (1+2x_2)r\eta + 2x_2 r^2}{\eta-r} \phi_\phi(x_2) + (1+x_2 r\eta) \phi_\phi^t(x_2) + x_2 r\sqrt{\eta^2-1} \phi_\phi^s(x_2) \right] \cdot H_1(t_1) \right. \\
& + \left[ \left[ r - \frac{x_1}{2} (\eta + \sqrt{\eta^2-1}) \right] \phi_\phi(x_2) + (x_1 + 2r\sqrt{\eta^2-1}) \phi_\phi^s(x_2) \right] \cdot H_2(t_2) \Big\}, \tag{A7}
\end{aligned}$$

where  $r = m_\phi/m_{B_s}$ , the twist-2 DAs ( $\phi_\phi, \phi_\phi^T$ ) and the twist-3 DAs  $\phi_\phi^{s,t}$  and  $\phi_\phi^{v,a}$  have been defined in Eqs. (7,9). The function  $H_i(t_i)$  in above equations are of the following form

$$H_i(t_i) = h_i(x_1, x_2, b_1, b_2) \cdot \alpha_s(t_i) \cdot S_t(x_2) \exp[-S_{ab}(t_i)], \quad \text{for } i = (1, 2). \tag{A8}$$

The hard functions  $h_{1,2}(x_1, x_2, b_1, b_2)$  come from the Fourier transform of virtual quark and gluon propagators and they can be defined by

$$\begin{aligned}
h_1 &= K_0(\beta_1 b_1) [\theta(b_1 - b_2) I_0(\alpha_1 b_2) K_0(\alpha_1 b_1) + \theta(b_2 - b_1) I_0(\alpha_1 b_1) K_0(\alpha_1 b_2)], \\
h_2 &= K_0(\beta_2 b_1) [\theta(b_1 - b_2) I_0(\alpha_2 b_2) K_0(\alpha_2 b_1) + \theta(b_2 - b_1) I_0(\alpha_2 b_1) K_0(\alpha_2 b_2)], \tag{A9}
\end{aligned}$$

where  $K_0$  and  $I_0$  are modified Bessel functions, and

$$\alpha_1 = m_{B_s} \sqrt{x_2 r \eta^+}, \quad \alpha_2 = m_{B_s} \sqrt{x_1 r \eta^+ - r^2 + r_s^2}, \quad \beta_1 = \beta_2 = m_{B_s} \sqrt{x_1 x_2 r \eta^+}, \tag{A10}$$

where  $r = m_\phi/m_{B_s}$ ,  $r_s = m_s/m_{B_s}$ . The hard scales  $t_i$  in Eq. (A8) are chosen as the largest scale of the virtuality of the internal particles in the hard  $b$ -quark decay diagram, including  $1/b_i$  ( $i = 1, 2$ ):

$$t_1 = \max\{\alpha_1, 1/b_1, 1/b_2\}, \quad t_2 = \max\{\alpha_2, 1/b_1, 1/b_2\}. \quad (\text{A11})$$

The threshold resummation factor  $S_t(x)$  in Eq. (A8) is adopted from [91],

$$S_t = \frac{2^{1+2c}\Gamma(3/2+c)}{\sqrt{\pi}\Gamma(1+c)}[x(1-x)]^c, \quad (\text{A12})$$

with a fitted parameter  $c(Q^2) = 0.04Q^2 - 0.51Q + 1.87$  [36] and  $Q^2 = m_{B_s}^2(1-r^2)$  [92]. The function  $S_t(x)$  is normalized to unity. The function  $\exp[-S_{ab}(t)]$  in Eq. (A8) contains the Sudakov logarithmic corrections and the renormalization group evolution effects of both the wave functions and the hard scattering amplitude, for more details of function  $\exp[-S_{ab}(t)]$  one can see Refs. [34, 91].

- 
- [1] B. Dey [LHCb Collaboration], *Lepton Flavor Universality tests in  $b \rightarrow sl^+l^-$  decays at LHCb*, PoS ICHEP **2018**, 069 (2019).
  - [2] R. Aaij *et al.* [LHCb Collaboration], *Test of lepton universality using  $B^+ \rightarrow K^+l^+l^-$  decays*, Phys. Rev. Lett. **113**, 151601 (2014).
  - [3] R. Aaij *et al.* [LHCb Collaboration], *Test of lepton universality with  $B^0 \rightarrow K^{*0}l^+l^-$  decays*, JHEP **1708**, 055 (2017).
  - [4] M. Bordone, G. Isidori and A. Pattori, *On the Standard Model predictions for  $R_K$  and  $R_{K^*}$* , Eur. Phys. J. C **76**, 440 (2016).
  - [5] G. Hiller and F. Kruger, *More model-independent analysis of  $b \rightarrow s$  processes*, Phys. Rev. D **69**, 074020 (2004).
  - [6] G. Hiller and M. Schmaltz, *Diagnosing lepton-nonuniversality in  $b \rightarrow sl\bar{l}$  test*, JHEP **02**, 055 (2015).
  - [7] S. Descotes-Genon, J. Matias and J. Virto, *Understanding the  $B \rightarrow K^*\mu^+\mu^-$  anomaly*, Phys. Rev. D **88**, 074002 (2013).
  - [8] J. Matias, F. Mescia, M. Ramon and J. Virto, *Complete Anatomy of  $\bar{B}_d \rightarrow \bar{K}^{*0}(\rightarrow K\pi)l^+l^-$  and its angular distribution*, JHEP **1204**, 104 (2012).
  - [9] J. Matias and N. Serra, *Symmetry relations between angular observables in  $B^0 \rightarrow K^*\mu^+\mu^-$  and the LHCb  $P'_5$  anomaly*, Phys. Rev. D **90**, 034002 (2014).
  - [10] S. Descotes-Genon, J. Matias, M. Ramon and J. Virto, *Implications from clean observables for the binned analysis of  $B \rightarrow K^*\mu^+\mu^-$  at large recoil*, JHEP **1301**, 048 (2013).
  - [11] S. Descotes-Genon, T. Hurth, J. Matias and J. Virto, *Optimizing the basis of  $B \rightarrow K^*ll$  observables in the full kinematic range*, JHEP **1305**, 137 (2013).
  - [12] R. Aaij *et al.* [LHCb Collaboration], *Measurement of Form-Factor-Independent Observables in the Decay  $B^0 \rightarrow K^{*0}\mu^+\mu^-$* , Phys. Rev. Lett. **111**, 191801 (2013).
  - [13] R. Aaij *et al.* [LHCb Collaboration], *Angular analysis of the  $B^0 \rightarrow K^{*0}\mu^+\mu^-$  decay using  $3\text{ fb}^{-1}$  of integrated luminosity*, JHEP **1602**, 104 (2016).
  - [14] A. Abdesselam *et al.* [Belle], *Angular analysis of  $B^0 \rightarrow K^*(892)^0\ell^+\ell^-$* , [arXiv:1604.04042 [hep-ex]].

- [15] S. Descotes-Genon, L. Hofer, J. Matias and J. Virto, *On the impact of power corrections in the prediction of  $B \rightarrow K^* \mu^+ \mu^-$  observables*, JHEP **1412**, 125 (2014).
- [16] A. Deandrea and A. D. Polosa, *The Exclusive  $B_s \rightarrow \phi \mu^+ \mu^-$  process in a constituent quark model*, Phys. Rev. D **64**, 074012 (2001).
- [17] S. Dubnicka, A. Z. Dubnickova, A. Issadykov, M. A. Ivanov, A. Liptaj and S. K. Sakhiyev, *Decay  $B_s \rightarrow \phi \ell^+ \ell^-$  in covariant quark model*, Phys. Rev. D **93**, 094022 (2016).
- [18] C. Q. Geng and C. C. Liu, *Study of  $B_s \rightarrow (\eta, \eta', \phi) \ell \bar{\ell}$  decays*, J. Phys. G **29**, 1103 (2003).
- [19] C. Bobeth, G. Hiller and G. Piranishvili, *CP Asymmetries in  $\bar{B} \rightarrow \bar{K}^*(\rightarrow \bar{K} \pi) \ell \bar{\ell}$  and Untagged  $\bar{B}_s, B_s \rightarrow \phi(\rightarrow K^+ K^-) \ell \bar{\ell}$  Decays at NLO*, JHEP **0807**, 106 (2008).
- [20] P. Ball and R. Zwicky,  *$B_{d,s} \rightarrow \rho, \omega, K^*, \phi$  decay form-factors from light-cone sum rules revisited*, Phys. Rev. D **71**, 014029 (2005).
- [21] Y. L. Wu, M. Zhong and Y. B. Zuo,  *$B_s, D_s \rightarrow \pi, K, \eta, \rho, K^*, \omega, \phi$  Transition Form Factors and Decay Rates with Extraction of the CKM parameters  $|V_{ub}|, |V_{cs}|, |V_{cd}|$* , Int. J. Mod. Phys. A **21**, 6125 (2006).
- [22] W. Altmannshofer and D. M. Straub, *New physics in  $b \rightarrow s$  transitions after LHC run I*, Eur. Phys. J. C **75**, 382 (2015).
- [23] A. Bharucha, D. M. Straub and R. Zwicky,  *$B \rightarrow V \ell^+ \ell^-$  in the Standard Model from light-cone sum rules*, JHEP **1608**, 098 (2016).
- [24] J. Gao, C.D. Lü, Y.L. Shen, Y.M. Wang and Y.B. Wei, *Precision calculations of  $B \rightarrow V$  form factors from soft-collinear effective theory sum rules on the light-cone*, Phys. Rev. D **101**, 074035 (2020).
- [25] S. Descotes-Genon, L. Hofer, J. Matias and J. Virto, *Global analysis of  $b \rightarrow s \ell \ell$  anomalies*, JHEP **1606**, 092 (2016).
- [26] R. Mohanta and A. K. Giri, *Study of FCNC mediated rare  $B_s$  decays in a single universal extra dimension scenario*, Phys. Rev. D **75**, 035008 (2007).
- [27] Y. Li and J. Hua, *Study of  $B_s \rightarrow \phi \ell^+ \ell^-$  Decay in a Single Universal Extra Dimension*, Eur. Phys. J. C **71**, 1764 (2011).
- [28] Y. G. Xu, L. H. Zhou, B. Z. Li and R. M. Wang, *Analysis of  $B_s \rightarrow \phi \mu^+ \mu^-$  decay within supersymmetry*, Chin. Phys. C **37**, 063104 (2013).
- [29] T. Aaltonen *et al.* [CDF Collaboration], *Measurement of the Forward-Backward Asymmetry in the  $B \rightarrow K^{(*)} \mu^+ \mu^-$  Decay and First Observation of the  $B_s^0 \rightarrow \phi \mu^+ \mu^-$  Decay*, Phys. Rev. Lett. **106**, 161801 (2011).
- [30] R. Aaij *et al.* [LHCb Collaboration], *Differential branching fraction and angular analysis of the decay  $B_s^0 \rightarrow \phi \mu^+ \mu^-$* , JHEP **1307**, 084 (2013).
- [31] R. Aaij *et al.* [LHCb Collaboration], *Angular analysis and differential branching fraction of the decay  $B_s^0 \rightarrow \phi \mu^+ \mu^-$* , JHEP **1509**, 179 (2015).
- [32] S. P. Jin, X. Q. Hu and Z. J. Xiao, *Study of  $B_s \rightarrow K^{(*)} \ell^+ \ell^-$  decays in the PQCD factorization approach with lattice QCD input*, Phys. Rev. D **102**, 013001 (2020).
- [33] Y. Y. Kim, H.N. Li and A.I. Sanda, *Penguin enhancement and  $B \rightarrow K \pi$  decays in perturbative QCD*, Phys. Rev. D **63**, 054008 (2001).
- [34] C. D. Lu, K. Ukai and M. Z. Yang, *Branching ratio and CP violation of  $B \rightarrow \pi \pi$  decays in perturbative QCD approach*, Phys. Rev. D **63**, 074009 (2001).
- [35] H. N. Li, *QCD Aspects of Exclusive B Meson Decays*, Prog.Part. & Nucl. Phys. **51**, 85 (2003) and references therein.
- [36] H. N. Li and S. Mishima, *Pion transition form factor in  $k_T$  factorization*, Phys. Rev. D **80**, 074024 (2009).

- [37] Y. Y. Fan, W. F. Wang, S. Cheng and Z. J. Xiao, *Anatomy of  $B \rightarrow K\eta^{(\prime)}$  decays in different mixing schemes and effects of next-to-leading order contributions in the perturbative QCD approach*, Phys. Rev. D **87**, 094003 (2013).
- [38] Y. Y. Fan, W. F. Wang, S. Cheng and Z. J. Xiao, *Semileptonic decays  $B \rightarrow D^{(*)}l\nu$  in the perturbative QCD factorization approach*, Chin. Sci. Bull. **59**, 125 (2014).
- [39] Z. J. Xiao, W. F. Wang and Y. Y. Fan, *Revisiting the pure annihilation decays  $B_s \rightarrow \pi^+\pi^-$  and  $B^0 \rightarrow K^+K^-$ : the data and the pQCD predictions*, Phys. Rev. D **85**, 094003 (2012).
- [40] W. F. Wang and Z. J. Xiao, *The semileptonic decays  $B/B_s \rightarrow (\pi, K)(\ell^+\ell^-, \ell\nu, \nu\bar{\nu})$  in the perturbative QCD approach beyond the leading-order*, Phys. Rev. D **86**, 114025 (2012).
- [41] W. F. Wang, Y. Y. Fan, M. Liu and Z. J. Xiao, *Semileptonic decays  $B/B_s \rightarrow (\eta, \eta', G)(\ell^+\ell^-, \ell\bar{\nu}, \nu\bar{\nu})$  in the perturbative QCD approach beyond the leading order*, Phys. Rev. D **87**, 097501 (2013).
- [42] A. Ali, G. Kramer, Y. Li, C. D. Lu, Y. L. Shen, W. Wang and Y. M. Wang, *Charmless non-leptonic  $B_s$  decays to  $PP$ ,  $PV$  and  $VV$  final states in the pQCD approach*, Phys. Rev. D **76**, 074018 (2007).
- [43] D. C. Yan, P. Yang, X. Liu, and Z. J. Xiao, *Anatomy of  $B_s \rightarrow PV$  decays and effects of next-to-leading order contributions in the perturbative QCD factorization approach*, Nucl. Phys. B **931**, 79 (2018).
- [44] D. C. Yan, X. Liu, and Z. J. Xiao, *Anatomy of  $B_s \rightarrow VV$  decays and effects of next-to-leading order contributions in the perturbative QCD factorization approach*, Nucl. Phys. B **935**, 17 (2018).
- [45] P. Ball, V. M. Braun and A. Lenz, *Higher-twist distribution amplitudes of the  $K$  meson in QCD*, JHEP **0605**, 004 (2006).
- [46] G. Buchalla, A. J. Buras and M. E. Lautenbacher, *Weak decays beyond leading logarithms*, Rev. Mod. Phys. **68**, 1125 (1996).
- [47] R. H. Li, C. D. Lu, W. Wang and X. X. Wang,  *$B \rightarrow S$  Transition Form Factors in the PQCD approach*, Phys. Rev. D **79**, 014013 (2009).
- [48] S. R. Singh and B. Mawlong,  *$331$ - $Z'$  mediated FCNC effects on  $b \rightarrow d\mu^+\mu^-$  transitions*, Int. J. Mod. Phys. A **33**, 1850225 (2019).
- [49] B. Kindra and N. Mahajan, *Predictions of angular observables for  $\bar{B}_s \rightarrow K^*\ell\ell$  and  $\bar{B} \rightarrow \rho\ell\ell$  in the standard model*, Phys. Rev. D **98**, 094012 (2018).
- [50] P. Nayek, P. Maji and S. Sahoo, *Study of semileptonic decays  $B \rightarrow \pi\ell^+\ell^-$  and  $B \rightarrow \rho\ell^+\ell^-$  in nonuniversal  $Z'$  model*, Phys. Rev. D **99**, 013005 (2019).
- [51] K. G. Chetyrkin, M. Misiak and M. Munz, *Weak radiative  $B$  meson decay beyond leading logarithms*, Phys. Lett. B **400**, 206 (1997).
- [52] K. G. Chetyrkin, M. Misiak and M. Munz,  *$|\Delta F| = 1$  nonleptonic effective Hamiltonian in a simpler scheme*, Nucl. Phys. B **520**, 279 (1998).
- [53] P. Gambino, M. Gorbahn and U. Haisch, *Anomalous dimension matrix for radiative and rare semileptonic  $B$  decays up to three loops*, Nucl. Phys. B **673**, 238 (2003).
- [54] C. Bobeth, M. Misiak and J. Urban, *Photonic penguins at two loops and  $m_t$  dependence of  $BR(B \rightarrow X_s l^+ l^-)$* , Nucl. Phys. B **574**, 291 (2000).
- [55] C. H. Chen and C. Q. Geng, *Baryonic rare decays of  $\Lambda(b) \rightarrow \Lambda l^+ l^-$* , Phys. Rev. D **64**, 074001 (2001).
- [56] C. S. Lim, T. Morozumi and A. I. Sanda, *A Prediction for  $d\Gamma(b \rightarrow s\ell\bar{\ell})/dq^2$  Including the Long Distance Effects*, Phys. Lett. B **218**, 343 (1989).
- [57] N. G. Deshpande, J. Trampetic and K. Panose, *Resonance Background to the Decays  $b \rightarrow$*

- $s\ell^+\ell^-$ ,  $B \rightarrow K^*\ell^+\ell^-$  and  $B \rightarrow K\ell^+\ell^-$ , Phys. Rev. D **39**, 1461 (1989).
- [58] A. Ali, T. Mannel and T. Morozumi, *Forward backward asymmetry of dilepton angular distribution in the decay  $b \rightarrow s\ell^+\ell^-$* , Phys. Lett. B **273**, 505 (1991).
  - [59] P. J. O'Donnell and H. K. K. Tung, *Resonance contributions to the decay  $b \rightarrow s\ell^+\ell^-$* , Phys. Rev. D **43**, 2067 (1991).
  - [60] A. Khodjamirian, Th. Mannel, A.A. Pivovarov and Y.M. Wang, *Charm-loop effect in  $B \rightarrow K^{(*)}l^+l^-$  and  $B \rightarrow K^*\gamma$* , JHEP **09**, 089 (2010).
  - [61] A. Khodjamirian, Th. Mannel, A.A. Pivovarov and Y.M. Wang,  *$B \rightarrow Kl^+l^-$  decay at large hadronic recoil*, JHEP **02**, 010 (2013).
  - [62] I. Ahmed, M. J. Aslam and M. Ali Paracha, *Impact of  $Z'$  and universal extra dimension parameters on different asymmetries in  $B_s \rightarrow \phi\ell^+\ell^-$  decays*, Phys. Rev. D **88**, no. 1, 014019 (2013).
  - [63] W. Altmannshofer, P. Ball, A. Bharucha, A. J. Buras, D. M. Straub and M. Wick, *Symmetries and Asymmetries of  $B \rightarrow K^*\mu^+\mu^-$  Decays in the Standard Model and Beyond*, JHEP **0901**, 019 (2009).
  - [64] D. Becirevic and E. Schneider, *On transverse asymmetries in  $B \rightarrow K^*l^+l^-$* , Nucl. Phys. B **854**, 321 (2012).
  - [65] U. Egede, T. Hurth, J. Matias, M. Ramon and W. Reece, *New physics reach of the decay mode  $\bar{B} \rightarrow \bar{K}^{*0}\ell^+\ell^-$* , JHEP **1010**, 056 (2010).
  - [66] U. Egede, T. Hurth, J. Matias, M. Ramon and W. Reece, *New observables in the decay mode  $\bar{B}_d \rightarrow \bar{K}^{*0}\ell^+\ell^-$* , JHEP **0811**, 032 (2008).
  - [67] M. Tanabashi *et al.* [Particle Data Group], *Review of Particle Physics*, Phys. Rev. D **98**, 030001 (2018).
  - [68] Y.M. Wang and Y.L. Shen, *QCD corrections to  $B \rightarrow \pi$  form factors from light-cone sum rules*, Nucl. Phys. B **898**, 563 (2015).
  - [69] F. Kruger and J. Matias, *Probing new physics via the transverse amplitudes of  $B^0 \rightarrow K^{*0}(\rightarrow K^-\pi^+)l^+l^-$  at large recoil*, Phys. Rev. D **71**, 094009 (2005).
  - [70] J. Gratrex, M. Hopfer and R. Zwicky, *Generalised helicity formalism, higher moments and the  $B \rightarrow K_{JK}(\rightarrow K\pi)\bar{l}_1l_2$  angular distributions*, Phys. Rev. D **93**, 054008 (2016).
  - [71] H. Y. Cheng, C. K. Chua and C. W. Hwang, *Covariant light-front approach for  $s$ -wave and  $p$ -wave mesons: its application to decay constants and form factors*, Phys. Rev. D **69**, 074025 (2004).
  - [72] W. Wang, Y. L. Shen and C. D. Lu, *Covariant light-front approach for  $B_c$  transition form factors*, Phys. Rev. D **79**, 054012 (2009).
  - [73] Y. Y. Fan, Z. J. Xiao, R. M. Wang and B. Z. Li, *The  $B \rightarrow D^{(*)}l\nu_l$  decays in the  $p$ QCD approach with the Lattice QCD input*, Sci. Bull. **60** (2015) 2009-2015.
  - [74] X. Q. Hu, S. P. Jin and Z. J. Xiao, *Semileptonic decays  $B_c \rightarrow (\eta_c, J/\psi)l\bar{\nu}_l$  in the "PQCD + Lattice" approach*, Chin. Phys. C **44** (2020) 023104.
  - [75] X. Q. Hu, S. P. Jin and Z. J. Xiao, *Semileptonic decays  $B/B_s \rightarrow (D^{(*)}, D_s^{(*)})l\nu_l$  in the PQCD factorization approach with the lattice QCD input*, Chin. Phys. C **44** (2020) 053102.
  - [76] C. Bourrely, I. Caprini and L. Lellouch, *Model-independent description of  $B \rightarrow \pi l\nu$  decays and a determination of  $|V_{ub}|$* , Phys. Rev. D **79**, 013008 (2009). [Erratum *ibid.* **82**, 099902 (2010)].
  - [77] D. Leljak, B. Melic and M. Patra, *On lepton flavour universality in semileptonic  $B_c \rightarrow \eta_c, J/\Psi$  decays*, JHEP **05**, 094 (2019).
  - [78] R. R. Horgan, Z. Liu, S. Meinel and M. Wingate, *Lattice QCD calculation of form factors*

- describing the rare decays  $B \rightarrow K^* \ell^+ \ell^-$  and  $B_s \rightarrow \phi \ell^+ \ell^-$ , Phys. Rev. D **89**, 094501 (2014).
- [79] C. D. Lu, Y. L. Shen, Y. M. Wang and Y. B. Wei, *QCD calculations of  $B \rightarrow \pi, K$  form factors with higher-twist corrections*, JHEP **1901**, 024 (2019).
  - [80] A. Bharucha, T. Feldmann and M. Wick, *Theoretical and Phenomenological Constraints on Form Factors for Radiative and Semi-Leptonic B-Meson Decays*, JHEP **1009**, 090 (2010).
  - [81] D. Bigi and P. Gambino, *Revisiting  $B \rightarrow D \ell \nu$* , Phys. Rev. D **94**, 094008 (2016)
  - [82] R. H. Li, C. D. Lu and W. Wang, *Transition form factors of  $B$  decays into  $p$ -wave axial-vector mesons in the perturbative QCD approach*, Phys. Rev. D **79**, 034014 (2009).
  - [83] U. O. Yilmaz, *Analysis of  $B_s \rightarrow \phi \ell^+ \ell^-$  decay with new physics effects*, Eur. Phys. J. C **58**, 555 (2008).
  - [84] Y. Q. Peng and M. Z. Yang, *Study of semileptonic decay of  $\bar{B}_s^0 \rightarrow \phi \ell^+ \ell^-$  in QCD sum rule*, arXiv:2001.08459 [hep-ph].
  - [85] D. Melikhov and B. Stech, *Weak form-factors for heavy meson decays: An Update*, Phys. Rev. D **62**, 014006 (2000).
  - [86] R. N. Faustov and V. O. Galkin, *Rare  $B_s$  decays in the relativistic quark model*, Eur. Phys. J. C **73**, 2593 (2013)
  - [87] C. D. Lu, W. Wang and Z. T. Wei, *Heavy-to-light form factors on the light cone*, Phys. Rev. D **76**, 014013 (2007).
  - [88] F. Su, Y. L. Wu, C. Zhuang and Y. B. Yang, *Charmless  $B_s \rightarrow PP, PV, VV$  Decays Based on the Six-Quark Effective Hamiltonian with Strong Phase Effects II*, Eur. Phys. J. C **72**, 1914 (2012).
  - [89] B. Aubert *et al.* [BaBar Collaboration], *Direct CP, Lepton Flavor and Isospin Asymmetries in the Decays  $B \rightarrow K^{(*)} \ell^+ \ell^-$* , Phys. Rev. Lett. **102**, 091803 (2009)
  - [90] S. Descotes-Genon and J. Virto, *Time dependence in  $B \rightarrow V \ell \ell$  decays*, JHEP **1504**, 045 (2015), Erratum: [ JHEP **1507**, 049 (2015) ].
  - [91] T. Kurimoto, H. N. Li and A. I. Sanda, *Leading power contributions to  $B \rightarrow \pi, \rho$  transition form-factors*, Phys. Rev. D **65**, 014007 (2002).
  - [92] W. F. Wang, H. N. Li, W. Wang and C. D. Lu, *S-wave resonance contributions to the  $B_{(s)}^0 \rightarrow J/\psi \pi^+ \pi^-$  and  $B_s \rightarrow \pi^+ \pi^- \mu^+ \mu^-$  decays*, Phys. Rev. D **91**, 094024 (2015).